Towards Fabrication of Corona-Free Nanoparticles

M.Sc. Thesis

By

Sachin Vishwakarma

DISCIPLINE OF CHEMISTRY

INDIAN INSTITUTE OF TECHNOLOGY INDORE

May 2024

Towards Fabrication of Corona-Free Nanoparticles

A THESIS

Submitted in partial fulfillment of the requirements for the award of the degree
of
Master of Science

by
Sachin Vishwakarma

DISCIPLINE OF CHEMISTRY
INDIAN INSTITUTE OF TECHNOLOGY INDORE
May 2024

INDIAN INSTITUTE OF TECHNOLOGY INDORE

CANDIDATE'S DECLARATION

I hereby certify that the work being presented in the thesis entitled '**TOWARDS FABRICATION OF CORONA-FREE NANOPARTICLE'** in the partial fulfillment of the requirements for the award of the degree of **MASTER OF SCIENCE** and submitted in the **DISCIPLINE OF CHEMISTRY, Indian Institute of Technology Indore**, is an authentic record of my work carried out during the time from July 2023 to May 2024 under the supervision of Prof. Anjan Chakraborty, Professor, IIT Indore.

I have not submitted the matter presented in this thesis for the award of any other degree of this or any other institute.

08/05/2024

Signature of the student with the date
Sachin Vishwakarma

This is to certify that the above statement by the candidate is correct to the best of my knowledge.

A Chakraborty 8/5/2024

Signature of the Supervisor of
M.Sc. thesis (with date)
Prof. Anjan Chakraborty

Sachin Vishwakarma has successfully given his M.Sc. Oral Examination held on
8th May 2024

A Chakraborty 8/5/2024

Signature of Supervisor of MSc thesis
Prof. Anjan Chakraborty
Date:

Convener, DPGC
Dr. Umesh A. Kshirsagar
Date:

Acknowledgments

I am deeply grateful to **Prof. Anjan Chakraborty**, my thesis supervisor at IIT Indore's Chemistry Department. His unwavering support and infectious enthusiasm were instrumental in navigating my M.Sc. research journey. Prof. Chakraborty's dedication to our research group inspired me to strive for excellence. Under his esteemed guidance, I completed my project, and his encouragement motivated me at every step. I am fortunate to have had such a mentor during this pivotal academic endeavor.

I extend my heartfelt appreciation to the members of the PSPC, **Prof. Satya S. Bulusu** and **Dr. Pravarthana Dhanpal**, for their invaluable insights and gracious support throughout my thesis work. Their guidance has enriched my academic experience and contributed significantly to fulfilling my research goals.

I am deeply grateful to **Ms. Huma Tabassum**, my project mentor, for her unwavering guidance and support throughout my research endeavor. Her expertise and encouragement have been invaluable, and I owe a special thanks for her continuous assistance and mentorship, which have significantly contributed to the success of my project.

Thank Mr. Debanjan Bagchi, Mr. Avijit Maity, Ms. Priyanka Nath, Mr. Khushwant Saini, Mr. Naveen Kumar, and Mr. Suman Choudhury for their constant support throughout this project.

Moreover, I am grateful to my family and friends for staying with me in my bad times.

Furthermore, I would like to express my admiration and gratitude to all my batchmates who have accompanied me on this journey. Their camaraderie, support, and shared experiences have made my M.Sc. journey memorable.

Sachin Vishwakarma
M.Sc. 2nd year

Dedication

To my beloved parents, this thesis is lovingly dedicated.

Abstract

The formation of a corona-free system of nanoparticles is an emerging field in nanoscience. When NPs are put into biological fluids, they gather a layer of biological material around them, called a "biological corona." This corona affects various biological processes, like how long the nanoparticles stay in circulation, how drugs are released from them, where they go in the body, and how they interact with cells inside the body. Because of these effects, AuNPs don't work as well as we'd like them to in things like delivering drugs to specific places, taking images inside the body, providing genes, and giving medicines. Various properties of gold nanoparticles and lipids have been extensively discussed in the literature up to this point. No report exists where aliphatic amino acid functionalized gold nanoparticles can form a stable and corona-free system. In our work, we aim to investigate the formation of the corona-free system on valine and isoleucine functionalized gold nanoparticles and to analyze how corona-free nanoparticles can boost their stability in the harsh environment of biological fluid. Our research findings indicate that gold nanoparticles functionalized with valine and isoleucine form a lipid corona, enhancing stability against external stimuli. These nanoparticles stabilize high-concentration favorable and zwitterionic lipid vesicles, whereas, at low concentrations, they undergo aggregation. The AuVal and AuILe NPs do not interact with negatively charged lipid vesicles, suggesting nanoparticles' negative surface charge. It has also been found that the nanoparticle's stability increases after the Lipid's coating around its Surface, i.e., lipid coating prevents nanoparticle aggregation in different environmental Conditions.

Table of Contents

List of Figures

List of Table

Nomenclature

° C	Degree Celsius
mL	Mililiter
mM	Milimolar
µL	Microliter
nm	Nanometer
nM	Nanomolar

Acronyms

AA	Amino Acid
NPs	Nanoparticles
AA-AuNPs	Amino Acid functionalized Gold Nanoparticles
DMPC	1,2-Dimyristoyl-sn-glycerol-3-phosphocholine
DPPC	1,2-dipalmitoylphosphatidylcholine
DOPC	1,2-dioleoyl-sn-glycerol-3-phosphocholine
DMPG	1,2-Dimyristoyl-sn-Glycerol-3- Phosphoglyceral sodium salt
DMTAP	2,3-di (tetradecanoyloxy) propyl-trimethylazanium Giant unilamellar Vesicle
$HAuCl_4$	Chlouroauric Acid
SPR	Surface Plasmon Resonance
Val	Valine
ILe	Isoleucine
AuVal NP	Valine Functionalized Gold Nanoparticle
AuILe NP	Isoleucine Functionalized Gold Nanoparticle

Literature Survey

The biomolecular corona, a dynamic layer of proteins and lipids on nanoparticles in biological fluids, alters their identity and impacts drug delivery. It can mask targeting ligands, hindering efficacy. Minimizing corona interference is crucial for precise targeting. Researchers are exploring surface engineering to optimize nanoparticle behavior and improve drug delivery[1].

Lagana et al. (2014) offer essential perspectives on developing nanoparticle-based delivery systems for cancer therapy, highlighting the significance of PEG chain length in controlling bio-nano interactions[2].

Rotello et al. (2014) investigate protein corona formation on NPs using zwitterionic NPs with adjustable hydrophobicity. These NPs resist protein adsorption at moderate serum protein levels and avoid hard coronas at physiological concentrations. This research enables the design of NPs for nanomedicine, enhancing interactions with biological systems and applications in targeted drug delivery and diagnostics[3].

Murphy et al. (2018) examine the spontaneous lipid corona formation around nanoparticles, which is crucial for understanding their interaction with biological systems. It reveals that contact ion pairing between nanoparticle ligands and lipid headgroups triggers this process, leading to changes in bilayer fluidity and particle characteristics[4].

Zhongjian et al. (2021) emphasize the efficacy of biological drugs despite poor membrane permeability. Liposomes act as drug carriers, enhancing stability, bioavailability, and effectiveness while reducing toxicity. Reviewing liposome types and clinical applications highlights their role in targeted drug delivery. Liposomes also show promise in delivering nucleic acids, addressing challenges like systemic clearance and enzymatic degradation in disease treatment[5].

Chakraborty et al. (2021) reported that zwitterionic lipid vesicles interact with gold nanoparticles functionalized with phenylalanine (AuPhe NPs),

resulting in the formation of a lipid corona that imparts stability to the nanoparticles against external stimuli.[6]. Recently, they examined the impact of lipid coronas on phenylalanine-functionalized gold nanoparticles (AuNPs). It reveals that lipid concentration influences corona formation and nanoparticle stability, pivotal for their biomedical application[7]. In our lab, our research explored the interaction between silver nanoparticles and lipid vesicles. We studied the formation of a lipid corona on silver nanoparticles and its effects on silver ion dissolution and nanoparticle aggregation. Silver nanoparticles functionalized with aromatic amino acids interact with lipid vesicles, exhibiting improved stability against pH variations, changes in salt concentration, and freeze-thaw cycles. Surface ligands play a critical role in lipid corona formation, offering insights for stable, lipid-coated nanoparticles in biomedical applications[8].

Developing a corona-free system for nanoparticles is critical in nanomedicine. The biomolecular corona forming around nanoparticles in biological fluids can alter their behavior, impacting drug delivery and cell interactions. Strategies like surface modifications and stealth coatings aim to prevent or minimize corona formation. This enhances nanoparticle precision and efficiency by reducing unwanted interactions. Achieving a corona-free system is essential for optimizing the effectiveness of nanoparticle-based therapies in biomedical applications. Our study focuses on understanding how aliphatic amino acid-functionalized gold nanoparticles interact with lipid vesicles to develop a corona-free system. This research aims to prevent the formation of a biomolecular corona around nanoparticles in biological environments, improving nanoparticle performance.

Chapter 1

Chapter 1: Introduction

1.1 Gold Nanoparticles: General Overview

Gold nanoparticles became a research focus in the late 19th and early 20th centuries, notably with Michael Faraday's experiments in 1857. Faraday's work with colloidal gold, where he created tiny gold particles suspended in liquid, marked the first scientific observation of these nanoparticles. He noticed the liquid turned red due to surface plasmon resonance. Throughout the 20th century, researchers like Richard Zsigmondy furthered their understanding of colloids and nanoparticles, laying the groundwork for future studies. However, it was in the late 20th and early 21st centuries that gold nanoparticles gained widespread attention and applications. Advances in synthesis and characterization methods led to discoveries of their potential in biomedicine, catalysis, electronics, and sensing[9-12]. This newfound interest propelled research into gold nanoparticles, leading to significant developments in various fields. Gold nanoparticles are super important in medicine, the environment, and electronics in the 21st century. They help deliver medicines better, clean up pollution, and make electronic gadgets work smarter. Their special properties make them key players in science and tech.

Gold nanoparticles, ranging from 1 to 100 nanometers, are prized for their unique qualities and many uses. They have surface plasmon resonance (SPR), making them great for medical imaging and sensing[13-15]. Because they're safe for living things and can be changed to fit specific needs, they're popular in medicine, especially for delivering drugs right where needed[16-17]. Gold nanoparticles are also stable and easy to modify, so they're handy in electronics, cleaning up the environment and helping chemical reactions happen[18-22]. People have studied them a lot, so we know how they work, making them a top choice for all scientific and tech stuff. Gold nanoparticles are liked more than other kinds because of their special properties, making them a top pick for all kinds of essential jobs in science and technology.

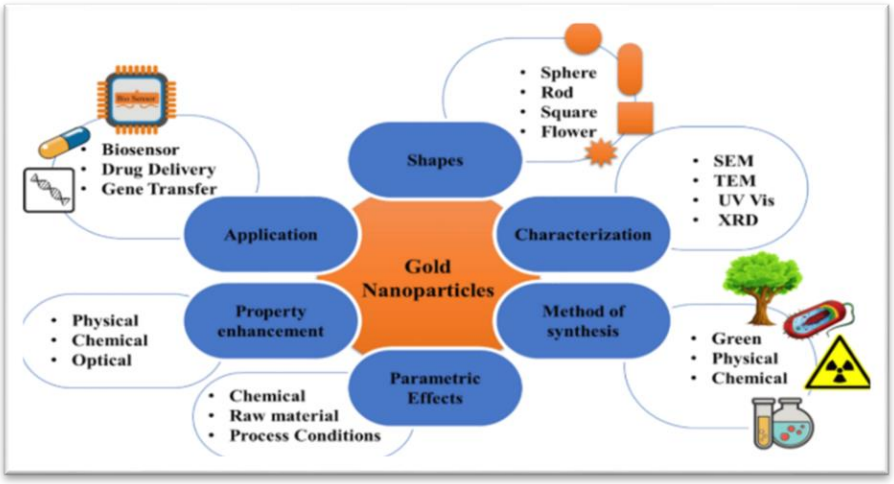

Figure 1: Application of Gold Nanoparticles[23].

Classification of Gold Nanoparticles:

Gold nanoparticles can be classified based on size, shape, synthesis method, and application. Standard classifications include spherical, nanorods, nanostars, nanocages, nanoshells, nanoclusters, and others. Synthesis methods include chemical reduction, seed-mediated growth, and green synthesis. Applications span biomedicine, catalysis, electronics, and environmental remediation.

Spherical Gold Nanoparticles: One of the most prevalent forms of synthesis involves creating symmetrical spherical AuNPs. These spherical AuNPs possess robust plasmonic characteristics and are utilized in catalysis, sensing, and biomedical applications.

Gold Nanoshell: Gold nanoshells consist of a dielectric core encased in a thin gold layer, offering tunable optical properties, especially in the near-infrared range. These characteristics render them highly useful for applications in biomedicine, including photothermal therapy, imaging, and drug delivery.

Gold Nanorod: Gold nanorods are elongated nanoparticles with unique optical properties due to their aspect ratio. They find applications in biomedical imaging, photothermal therapy, and sensing due to their tunable plasmonic resonance in the visible and near-infrared regions.

Gold Nanocluster: Gold nanoclusters are extremely small assemblies comprising a few to several gold atoms, showcasing distinctive photoluminescence properties. These nanoclusters are applied in imaging, sensing, and catalysis due to their high surface-to-volume ratio and adjustable fluorescence in visible and near-infrared spectra.

Gold Nanocage: Gold nanocages are hollow nanostructures with a porous lattice-like shell made of gold. They possess unique optical and catalytic properties, finding applications in biomedical imaging, drug delivery, and photothermal therapy due to their high surface area and tunable plasmonic resonance.

Gold Nanostar: Gold nanostars are nanoparticles characterized by multiple branches extending from a central core, resembling a star shape. They demonstrate robust localized surface plasmon resonance and are utilized in surface-enhanced Raman spectroscopy, photothermal therapy, and biosensing, leveraging their enhanced electromagnetic field properties and adjustable optical characteristics.

Spherical gold nanoparticles are commonly used in research and applications due to their uniform size, ease of synthesis, and well-understood properties. They exhibit plasmonic solid resonance, making them suitable for various optical and biomedical applications such as imaging, sensing, drug delivery, and catalysis.

Synthesis of Gold Nanoparticle:

The synthesis of gold nanoparticles involves various methods that allow researchers to control the nanoparticles' size, shape, and properties. Here's a simplified explanation of the synthesis process:

Chemical Reduction Method:

Gold nanoparticles are synthesized by reducing Au^{+3} ions to Au^{0} atoms using reducing agents like sodium citrate, sodium borohydride, amino acid, or ascorbic acid. Stabilizing agents, such as capping molecules or polymers, are introduced to prevent nanoparticle aggregation during the reduction reaction. This process allows for the controlled formation of gold

nanoparticles with desired properties for various applications like biomedicine, catalysis, and electronics[24].

Seed-Mediated Growth Method:

The seed-mediated growth method utilizes pre-formed gold nanoparticles, termed seeds, as templates for larger nanoparticle growth. These seeds are mixed with a gold ion precursor solution and a reducing agent. It is possible to adjust the size and shape of NP through meticulous control of reaction parameters such as temperature and pHs. This approach facilitates the custom synthesis of AuNPs with specific properties tailored for a wide range of applications in biomedicine, catalysis, and electronics. [25].

Green Synthesis Methods:

Green synthesis methods employ natural or biological agents like plant extracts, bacteria, or fungi as reducing and stabilizing agents in nanoparticle synthesis. These methods are environmentally friendly and offer advantages in biocompatibility and scalability. By utilizing renewable resources and reducing the need for harsh chemicals, green synthesis contributes to sustainable nanoparticle production for applications spanning biomedicine, catalysis, and environmental remediation[26].

Overall, synthesizing gold nanoparticles involves a combination of chemical reactions and physical processes that are carefully controlled to produce nanoparticles with desired properties for specific applications.

1.2 Synthesis of Nanoparticles

Nanoparticles, primarily composed of metals, are stabilized by ligands on their surface to prevent aggregation. Chemical synthesis methods involve metal salts, reducing agents, and stabilizing agents to form the nanoparticle core and maintain stability. Additionally, natural sources like plants and fungi are utilized for nanoparticle formation, offering eco-friendly alternatives with unique optical properties detectable by UV-Vis spectroscopy. Advanced characterization techniques such as TEM, SEM, and AFM provide insights into nanoparticle morphology and structure.

TEM offers high-resolution imaging, SEM reveals surface features, and AFM enables precise surface property measurements. These methods facilitate tailoring nanoparticle properties for diverse applications, including biomedical imaging, drug delivery, catalysis, and electronics. The multidisciplinary approach underscores nanoparticles' versatility and potential impact across various scientific domains[27].

1.3 Amino-Acid Functionalized Gold Nanoparticles

Aromatic amino acids, featuring -NH_2 and -COOH groups, play vital roles as stabilizing and reducing agents in synthesizing gold nanoparticles (AuNPs). In our investigation, we utilized aliphatic amino acids such as valine and isoleucine, complemented by including NaOH, to bolster their reducing capabilities. We discovered that the concentrations of amino acids and NaOH significantly influenced the size of the resulting AuNPs. Furthermore, temperature variations, whether at ambient or elevated levels, emerged as critical determinants affecting the kinetics of nanoparticle formation. These insights highlight the necessity of precise control over experimental variables such as amino acid concentration, NaOH concentration, and temperature to tailor the size and properties of AuNPs. Such meticulous control has profound implications for optimizing AuNPs synthesis protocols, enhancing their suitability for targeted applications in nanotechnology and biomedicine.

1.4 Dynamic Light Scattering (DLS) and Zeta Potential

The DLS data obtained from Dynamic Light Scattering analysis provides valuable insights into the characteristics of nanoparticles, particularly their size distribution and polydispersity. This information is crucial for understanding the uniformity or variation in nanoparticle sizes within a sample. The range of particle sizes in the sample and the size distribution data show their respective abundance or intensity. A narrow size distribution indicates similarity in size, while a broader distribution suggests diversity[28].

Measuring the zeta potential helps us understand the surface charge of nanoparticles (NPs). Zeta potential shows us the electric charge around the particles in a liquid. A higher positive or negative zeta potential means the particles repel each other more strongly, which stops them from sticking together. This information is essential for knowing how stable and spread the NPs will be in different uses. Analyzing the zeta potential gives us insights into the surface properties of NPs, like their charge and how they interact with other things in the liquid[29].

1.5 Lipid Bilayer

Liposomes, very small artificial vesicles composed of lipid bilayers, represent versatile carriers with applications from drug delivery to cosmetic formulations. Their structure consists of hydrophobic tails and hydrophilic heads, enabling them to form stable, spherical structures in aqueous environments[30]. Liposomes vary in size, ranging from micrometers to nanometers, depending on the specific formulation and intended use.

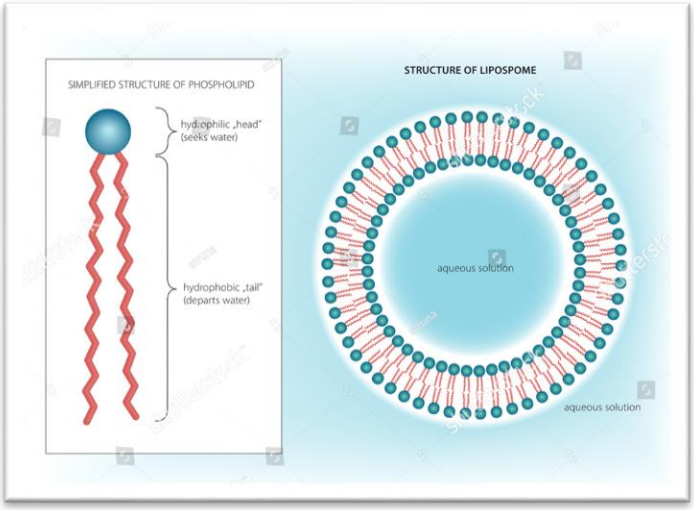

Figure 2: Lipid Bilayer[31].

One of the critical advantages of liposomes lies in their biocompatibility and non-toxic nature, making them ideal candidates for delivering drugs and other therapeutic agents in medicine. Liposomes protect the payload from

degradation by encapsulating drugs within their lipid bilayers or aqueous compartments and enhancing their bioavailability. Moreover, liposomes can be engineered to target specific tissues or cells, thereby improving the efficacy of treatments while minimizing side effects.

In addition to drug delivery, liposomes are useful in cosmetic formulations, carrying active ingredients such as vitamins, antioxidants, and moisturizers. Their ability to penetrate the skin barrier and deliver these compounds effectively makes them valuable components in skincare products. Liposomes are utilized as chemical carriers in medicine delivery systems since they are naturally non-toxic. The preparation of liposomes can be done in several ways. Some of the most popular techniques are the reverse phase evaporation method, the solvent injection method, and the thin-film hydration method. Several lipids (DMPC, DOPC, DPPC, DMTAP, and DMPG) have been employed to produce liposomes using solvent injection.

Overall, liposomes represent a promising platform for delivering therapeutic agents in a controlled and targeted manner, with potential applications in medicine, cosmetics, and beyond. Their versatility, biocompatibility, and ability to encapsulate various substances make them indispensable tools in modern healthcare and beauty industries.

1.6 Lipid Corona

A "lipid corona" refers to the layer of lipids that naturally forms around nanoparticles when introduced into biological fluids like blood or tissue fluid. This corona is created as lipid molecules from the fluid adhere to the surface of the nanoparticles due to their chemical properties. The composition and thickness of the lipid corona can vary depending on factors such as the type of nanoparticles, the surrounding biological environment, and the specific lipid molecules present. A lipid corona can influence various aspects of nanoparticle behavior, including stability, interaction with cells, circulation time in the bloodstream, immune response, potential

toxicity, and effectiveness in delivering drugs or imaging agents to target tissues[32-35].

A "lipid bilayer" is like the basic building block of cell membranes. It's made up of two layers of fat molecules. These fat molecules have two parts: one that hates water (hydrophobic) and another that loves water (hydrophilic). In the bilayer, the hydrophobic parts face each other inside, while the hydrophilic parts face outward, touching the watery environments inside and outside the cell. This arrangement forms a barrier separating the cell's inside from the outside. This flexible barrier can let some molecules pass through while keeping others out, like a gatekeeper. This helps the cell control what goes in and out, which is crucial for survival and functioning.

Many studies have looked at how nanoparticles interact with lipid bilayers, focusing on the role of the lipid headgroup in these interactions. Our previous research explored how different charged lipid vesicles interact with gold nanoparticles (AuNPs). We found that when more lipids were present, a stable coating formed around the AuNPs, making them stable. But when there was less lipid, the AuNPs clumped together, regardless of the lipid's charge. We're taking this research further by using other AA-AuNPs with the same coating, zwitterionic, and charged lipids. We want to see how these Aliphatic AA-AuNPs interact with lipids of varying charges to understand better how nanoparticles and lipids interact and form a coating around the NPs. This research is essential for advancing our understanding of how nanoparticles interact with biological systems, which could help us design better future drug delivery systems and other biomedical applications.

1.7 Effect of Lipid Coating on Stability of AuNPs

Lipid nanoparticles have emerged as promising drug delivery tools due to their remarkable biocompatibility and efficacy. One of the key factors contributing to their significance is their ability to enhance the stability of

nanoparticles through lipid coatings. While nanoparticles in their functinalized form may exhibit stability, they can encounter challenges in aqueous environments, potentially leading to toxic effects. Factors such as pH variations, changes in salt concentrations, different metal ions like Zn, Mg, and Cu, and fluctuations in temperature can further exacerbate nanoparticle instability by neutralizing surface charges, promoting oxidation, ion dissolution, or even aggregation of nanoparticles.

The lipid coating surrounding nanoparticles is a protective barrier, improving their biocompatibility and shielding them from adverse environmental conditions. This lipid layer provides robust stability to nanoparticles under diverse conditions, including variations in pH, salt concentrations, and freeze-thaw cycles. In our study, we aim to delve deeper into the impact of lipid coatings on nanoparticle stability by subjecting them to different pH levels, varying salt concentrations, and multiple freeze-thaw cycles. Understanding the role of lipid coatings in enhancing nanoparticle stability is crucial for optimizing drug delivery systems and ensuring their effectiveness across various physiological conditions.

This technique is well-known, where change the amount of salt and H^+ (hydrogen ions) in a solution to see how it affects the stability of nanoparticles. When there's a lot of H^+ and ions around, they tend to cancel out the charge on the surface of the nanoparticles, which makes them clump together or aggregate. But if the nanoparticles are coated with something, it can help stop this from happening as much. By adjusting the amounts of salt and H^+ in the solution, scientists can figure out how to make the nanoparticles stay stable for longer. This kind of study is essential because it helps us understand how to control nanoparticles better, which can be helpful in medicine and technology. By changing the concentration of both salt and H^+ (which affects the pH), we can fine-tune the conditions to get the best results.

1.7.2 Interaction with different Metal Ions:

We're investigating how AA-AuNPs behave when exposed to various metal ions like zinc (Zn), copper (Cu), and magnesium (Mg). Mixing the gold nanoparticles with solutions containing these metal ions, we observe whether they remain stable or aggregate. Stability is crucial for their effectiveness in applications such as medicine and technology. If the nanoparticles clump together, it indicates instability, potentially compromising their functionality. Understanding how different metal ions influence nanoparticle stability helps in optimizing their performance. This research sheds light on the interactions between gold nanoparticles and metal ions, aiding in developing more effective nanoparticle-based systems for various applications.

1.7.3 Freeze-Thaw Cycle:

The Freeze-Thaw Cycle is a simple way to check if nanoparticles are stable. Here's how it works: First, we cool down the nanoparticles to low temperatures to freeze them. Then, we bring them back to average temperature to thaw them out. When we freeze the nanoparticles, they get pushed aside by the water, turning into ice. This makes the area around the nanoparticles more crowded, which can help keep them stable[36].

We use this method to see how well the nanoparticles stay apart from each other. We can determine their stability by doing this cycle a few times and seeing how much the nanoparticles clump together each time. This is important because we want nanoparticles to stay separate so they can do their job correctly, like delivering medicine or helping with technology. So, by measuring how much the nanoparticles stick together after each freeze-thaw cycle, we can tell if they're stable or not.

1.8 Interaction of Protein

When gold nanoparticles interact with proteins in biological environments, a protein corona forms around the AuNP surface. Initially, proteins adsorb

onto the AuNP, driven by various electrostatic forces, hydrophobic interactions, and hydrogen bonding. This protein corona layer influences the biological fate of AuNPs, affecting their cellular uptake, distribution, and toxicity. The composition and structure of the protein corona are dynamic and dependent on factors like nanoparticle size, shape, and surface chemistry. Understanding protein corona formation is crucial for predicting and controlling the behavior of AuNPs in biological systems.

1.9 Objective

To comprehend our research aim, it's crucial to grasp the corona effect in nanoparticles. When nanoparticles encounter biological fluids like blood or cell culture media, they attract various molecules such as proteins and other biomolecules. These molecules can adsorb onto the nanoparticle surface, forming a "corona." This corona can alter the nanoparticles' properties and interactions with biological systems. By preventing the formation of a protein or lipid corona, nanoparticles can maintain their desired properties and functions, leading to improved therapeutic outcomes. Corona-free nanoparticles offer significant benefits, including increased stability and enhanced drug delivery.

We aim to functionalize gold nanoparticles with aliphatic amino acids and investigate their interactions with lipids and proteins to establish a corona-free system. This entails designing nanoparticles that resist corona formation, preserving their inherent characteristics, and optimizing their performance in biomedical applications. Through this research, we aim to contribute to developing more effective nanoparticle-based therapies with enhanced stability and efficacy.

Chapter 2

Chapter 2: Experimental Section

2.1 Chemical and Regents

We purchased two Amino Acids Valine (Val), Isoleucine (ILe), Chloroauric Acid($HAuCl_4$), and HEPES (4-(2-hydroxyethyl)-1-piperazineethanesulfonic acid, sodium chloride salt anhydrous, from Sigma-Aldrich. The phospholipids, i.e., DMTAP (2,3-di(tetradecanoyloxy) propyl-trimethylammonium chloride), DMPG (1,2-Dimyristoyl-sn-glycero-3-phosphorylglycerol sodium salt), DMPC (1,2-Dimyristoyl-sn-glycero-3-phosphocholine), DPPC (1,2-dipalmitoylphosphatidylcholine), DOPC (1,2-dioleoyl-sn-glycero-3-phosphocholine), and human serum albumin (HSA) calf thymus were purchased from Avanti Polar Lipids. NaOH (Sodium Hydroxide) and Milli-Q water were purchased from Merck. All these chemicals were used and received without further purification. All the glassware was kept overnight in aqua regia (HCl/HNO_3^- 3:1) and cleaned correctly before the experiments.

2.2 Synthesis of AA-AuNPs

We synthesized AuNPs in situ using two different aliphatic amino acids. We have synthesized colloidal and stable amino acid functionalized AuNPs by employing amino acid concentrations of 1 mM, gold salt concentration of 0.75 mM, and NaOH concentration of 0.10 mM.

To prepare AuNPs, we started by mixing 8.75 mL of Milli-Q water with 250 µL of a 0.75 mM aqueous gold solution. This mixture was then stirred continuously for 30 minutes at 80°C. Subsequently, a specific amount of amino acid solution at a defined concentration was added, followed by NaOH at the desired concentration. The solution was maintained at 80°C for 2 hours with continuous stirring. As the colloidal AuNPs formed, the color of the solution changed from colorless to wine red.

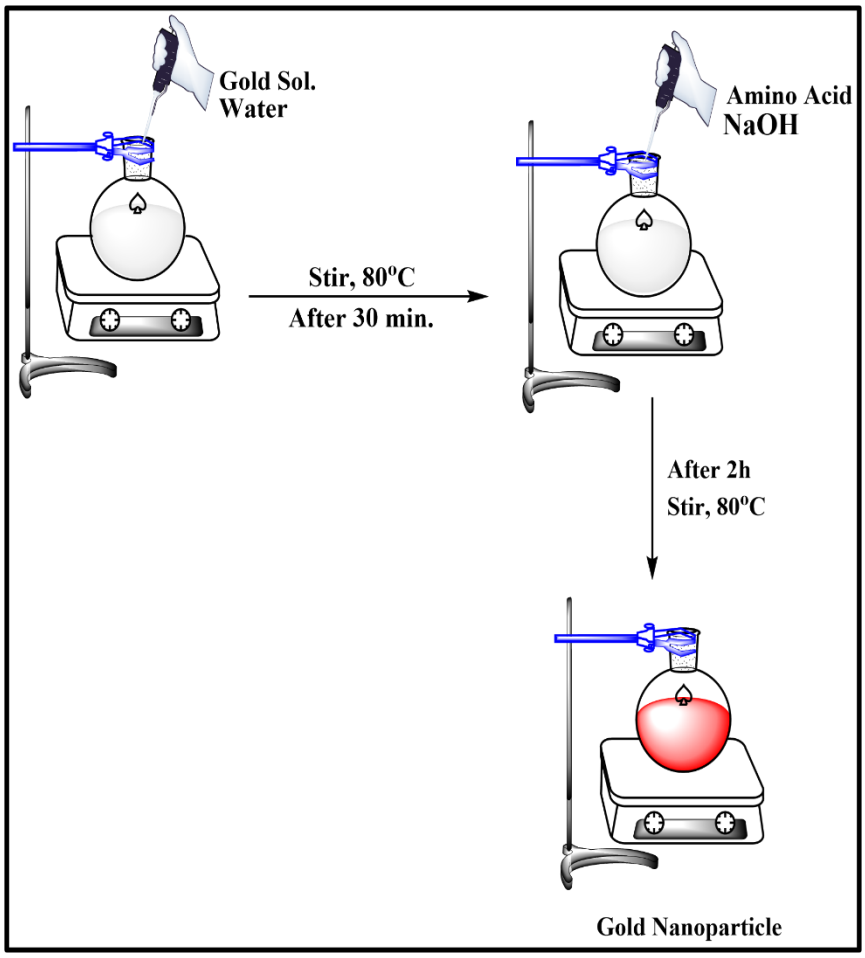

Figure 3: Process of Synthesis

2.3 Preparation of Supernatant Solution

We have taken 1 mL of our nanoparticle solution into the Eppendorf tube. Then, we put them in a centrifuge (REMI RM 12C BL) machine and let them spin fast for about 20 minutes. After spinning, we saw that the solution separated into two layers: at the bottom, there were the nanoparticles, and at the top, there was an unreacted solution called the supernatant. We carefully removed out 750 µL of the supernatant from the tube and added the same amount of HEPES to the tube.

Further experiments were done on the centrifuges AuNPs solution for each characterization.

2.4 Preparation of Nanoparticle sample for pH experiment

The stability of gold nanoparticles (AuNPs) under varying pH conditions was investigated through experiments conducted at both high and low pH levels. The pH of the AuNPs solution was systematically adjusted using sodium hydroxide for high pH and hydrochloric acid for low pH.

For this experiment, NaOH was used to achieve high pH, and HCl was utilized for low pH conditions. A total of 172µL was drawn from an 11.65N HCl stock solution to create a low-pH solution, and 1.828mL of water was added, resulting in a final concentration of 1M HCl. For the high-pH solution, 160mg of NaOH was placed in a vial, followed by the addition of 4 mL of water, resulting in a final concentration of 1M NaOH. Subsequently, 10µL of either HCl or NaOH were added to 1mL of the AuNPs solution, and the pH of the AuNPs was assessed using pH paper. If the desired pH was not attained, 10µL of NaOH or HCl was incrementally added until the desired pH was achieved. Subsequently, UV-Visible spectra of the AuNPs were obtained. This method allows for the controlled adjustment of pH in the AuNPs solution, facilitating a systematic study of the impact of pH on their properties.

2.5 Preparation of Nanoparticle sample for the salt experiment

In the experiment, 5.8 mg of sodium chloride (NaCl) was placed in an Eppendorf tube and then 1 mL of nanoparticle (NP) solution was added to it. The sample was incubated for 1 hour in an incubator for interaction. Subsequently, UV-Visible spectra were recorded to analyze any changes induced by the presence of NaCl. This method is utilized to understand how NaCl influences the optical properties of nanoparticles, providing insights into their stability and composition.

2.6 Preparation of Nanoparticle samples for different metal ions experiment

In this experiment, a 2mM, 10mL stock solution was prepared by combining specific amounts of calcium (Ca), magnesium (Mg), and zinc (Zn) salts with 10mL of HEPES buffer solution. For Ca, Mg, and Zn, 2.2 mg, 4.06 mg, and 2.72 mg were taken and dissolved in vials with 10mL of HEPES buffer, resulting in a 2mM concentration.

The nanoparticle stability was assessed at various concentrations (0.05mM, 0.1mM, 0.2mM, 0.5mM, and 1mM) of salts. 500mL of nanoparticle (NP) solutions were prepared in Eppendorf tubes to experiment. Simultaneously, salt samples were prepared by adding 25µL for 0.05mM, 50µL for 0.1mM, 100µL for 0.2mM, 25µL for 0.5mM, and 500µL for 1mM concentrations of salt into separate Eppendorf tubes.

To each of these salt samples, corresponding volumes of HEPES buffer solution were added 475µL, 450µL, 400µL, and 300µL for 0.05mM, 0.1mM, 0.2mM, and 0.5mM concentrations, respectively. The contents of the Eppendorf tubes were mixed thoroughly. Subsequently, the salt solutions were introduced into the NP solutions, and UV-Visible spectra were obtained for analysis. This experimental design allows for examining nanoparticle stability under different concentrations of salts, providing valuable insights into their interactions.

2.7 Preparation of Nanoparticle sample for the interaction of Protein

To conduct this experiment, a 20µM stock solution was meticulously prepared. This solution was created by combining 2.67mg of HSA protein with 2 mL of HEPES buffer, forming a 20µM stock solution. In the next step, an Eppendorf tube was employed to mix 500mL of the nanoparticle solution with 500mL of the protein solution. The resulting solution contained a protein concentration of 10µL. Following the preparation of the

sample, UV-Visible spectra of the solution were captured using sophisticated instrumentation.

2.8 Freeze-thaw cycle

In the freeze-thaw experiment, nanoparticle samples underwent freezing at -20^{o}C for 25 minutes, after which one sample was thawed at room temperature. Subsequent UV data acquisition captured the observed changes. The freezing process was followed by thawing at room temperature, and UV data collection was performed to analyze the resulting changes.

2.9 Preparation of Lipid Vesicles

In a HEPES medium with a pH of 7.42, all distinct liposome formulations with surface charges were prepared at a concentration of 0.8 mM. Initially, 3 ml of the HEPES solution was added to a round bottom flask and then heated to 80°C for approximately one hour. The required amount of lipid was subsequently added, and lipid dissolution was achieved using 1% ethanol. After one hour, the flask was left uncovered for ten to fifteen minutes to allow for the evaporation of ethanol. Subsequently, the heating was turned off, and the mixture was vigorously stirred for the whole night(~12h). A mixture of neutral DMPC and charged DMTAP/DMPG in a 7:3 ratio was utilized to mitigate potential repulsion between the charged lipids.

2.9.1 Lipid Vesicle-Nanoparticle Mixture Preparation:

We studied the formation of a lipid corona around AuNPs using different concentrations of lipid vesicles. The concentration of AuNPs was kept constant at approximately 5 nM, while the lipid concentration ranged from 0.8 mM to 0.0125 mM. In brief, 500 µL of AuNPs was placed in an Eppendorf tube, followed by the addition of 500 µL of varying lipid

concentrations. The mixture was then incubated for 10 hours at 30°C. The specific concentrations used are detailed in the table provided below.

Volume of NP	Volume of Lipid	The volume of the HEPES buffer	Concentration of Lipid in NPs
500 µL	500 µL	0 µL	0.8 mM
500 µL	250 µL	250 µL	0.4 mM
500 µL	125 µL	375 µL	0.2 mM
500 µL	62.5 µL	437.5 µL	0.1 mM
500 µL	31.25 µL	468.75 µL	0.05 mM
500 µL	15.62 µL	484.38 µL	0.025 mM
500 µL	7.8 µL	492.2 µL	0.0125 mM

Table 1: Lipid-Nanoparticles Sample Preparation

Concentration of Au-AA NPs (nM)	Number of Au-AA NPs /mL	Concentration of lipid (mM)	N_{tot}	N_{lipo}	Number ratio of Au-AA NPs: liposomes
5	1.204×10^{12}	0.8	97,389.01	4.938×10^{12}	1:4
5	1.204×10^{12}	0.4	97,389.01	2.469×10^{12}	1:2
5	1.204×10^{12}	0.2	97,389.01	1.236×10^{12}	1:1
5	1.204×10^{11}	0.1	97,389.01	6.184×10^{11}	2:1
5	1.204×10^{11}	0.05	97,389.01	3.092×10^{11}	4:1
5	1.204×10^{11}	0.025	97,389.01	1.546×10^{11}	8:1
5	1.204×10^{10}	0.0125	97,389.01	7.730×10^{10}	16:1

Table 2: Lipid-Nanoparticles Ratio Calculations

Chapter 3

Chapter 3: Results and Discussions

3.1 Optimization and characterization of aliphatic amino acid functionalized AuNPs

We aim to synthesize aliphatic amino acid functionalized gold nanoparticles (AA-AuNPs) using different aliphatic amino acids, namely **Alanine, Arginine, Asparagine, Aspartic acid, Cysteine, Glutamine, Glutamic acid, Glycine, Histidine, Isoleucine, Leucine, Lysine, Methionine, Proline, Serine, Threonine, Hydroxyproline, and Valine**. In this process, the amino acids serve dual functions as reducing and stabilizing agents. We synthesized all amino acid-functionalized AuNPs, and the results are as follows:

Au NP functionalized with	SPR Peak (nm)	Result
Alanine	534	Red
Arginine	535	Pink
Asparagine	518	Red
Aspartic Acid	516	Red
Cysteine	-	Colorless
Glutamine	527	Red
Glutamic Acid	535	Red
Glycine	525	Red
Histidine	537	Pink

Isoleucine	**521**	**Red**
Leucine	**527**	**Red**
Lysine	**554**	**Blue**
Methionine	**525**	**Red**
Proline	**542**	**Blue**
Serine	**533**	**Red**
Threonine	**526**	**Red**
Hydroxyproline	**519**	**Red**
Valine	**521**	**Red**

Table 3: All Synthesized AuNPs

Among all, five AuNPs are successfully synthesized, but Valine and isoleucine-functionalized gold nanoparticles demonstrate excellent properties, including a surface plasmon resonance (SPR) peak at **521 nm**, a size of about 12 nm, and a concentration of 5 nM. That is why they were chosen for further research. Valine has a straight-chain structure with a methyl group on the beta carbon. At the same time, Isoleucine features a branched structure with an additional methyl group on the beta carbon. These structural differences influence their roles in the synthesis process and contribute to the unique properties of the resulting AA-AuNPs. The Structure of these two aliphatic amino acids (AA) is given below-

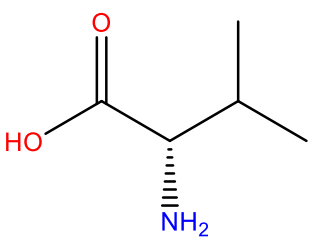

Valine

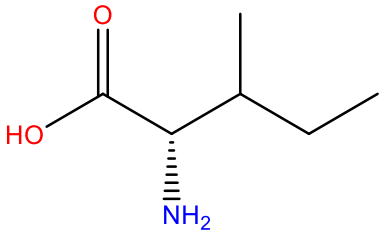

Isoleucine

As previously mentioned, the gold salt concentration remains at 0.75 mM, NaOH concentration at 0.10 mM, and amino acid concentration at 1 mM. These consistent concentrations were employed to synthesize both AA-AuNPs. Maintaining uniformity in these concentrations ensures standardized synthesis procedures, contributing to reliable and comparable outcomes in the production of the nanoparticles.

3.1.1 AuVal NP

It was observed that under optimized conditions (0.75 mM gold salt, 1 mM Valine, and 0.10 mM NaOH), Valine-functionalized gold nanoparticles with a size of approximately 12 nm were measured[37]. The UV-Visible spectra exhibited a surface plasmon resonance (SPR) peak at 521 nm, indicating the characteristic optical properties of the synthesized nanoparticles.

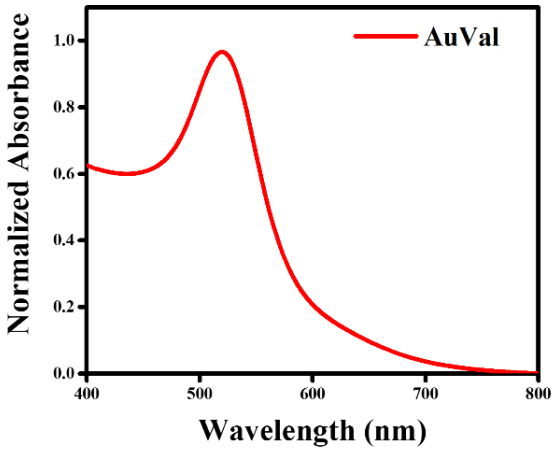

Figure 4: UV-Visible spectrum of AuVal NP

3.1.2 AuILe NP

It was observed that under optimized conditions (0.75 mM gold solution, 1 mM Valine, and 0.10 mM NaOH), Isoleucine-functionalized gold nanoparticles with a size of approximately 12 nm were measured. The UV-Visible spectra exhibited a surface plasmon resonance (SPR) peak at **521 nm**, indicating the characteristic optical properties of the synthesized nanoparticles.

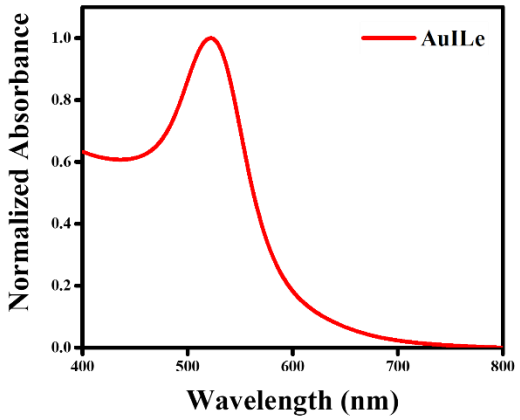

Figure 5: UV-Visible spectrum of AuILe NP

3.2 DLS data of AuNPs

The DLS measurements reveal that AuVal nanoparticles have an average hydrodynamic diameter of **30.62 nm**, whereas AuILe nanoparticles exhibit an average diameter of **34.18 nm** in solution. The larger size of AuILe compared to AuVal suggests that the presence of isoleucine as a coating leads to a thicker or more extended surface layer around the gold nanoparticles, resulting in increased hydrodynamic size. This size variation between AuVal and AuIle nanoparticles likely arises from differences in

their surface chemistry and interactions when coated with different amino acids. The choice of amino acid coating can significantly influence the nanoparticle's surface properties, including the thickness and structure of the surrounding layer, which in turn affects their overall size and behavior in solution.

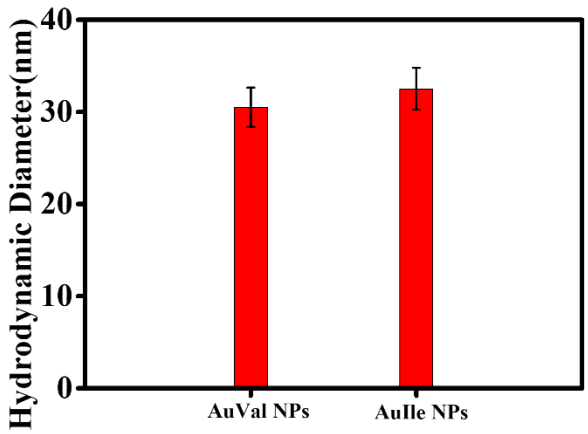

Figure 6: DLS of AuVal and AuILe NPs

3.3 Zeta Potential of AuNPs

The zeta potential measurements indicate that AuVal nanoparticles have a zeta potential of **-24.57 mV**, while AuIle nanoparticles have a zeta potential of **-27.67 mV** in solution. These zeta potential values reflect the surface charge of the NPs. The more negative zeta potential observed for AuIle compared to AuVal suggests that the isoleucine coating imparts a slightly higher negative charge to the nanoparticles. This difference in zeta potential could be attributed to variations in the surface chemistry and interactions between the nanoparticles and the surrounding solution, influenced by the specific amino acid used as a coating. The negative zeta potentials of both AuVal and AuIle nanoparticles indicate good stability and dispersion in the

solution, as the like charges on the particle surfaces repel each other, minimizing aggregation or clumping.

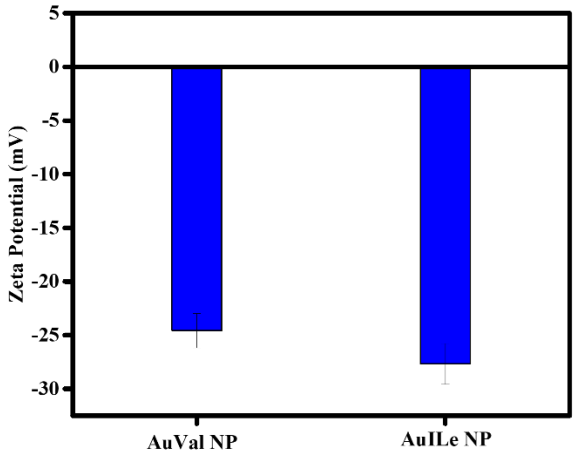

Figure 7: Zeta Potential of AuVal and AuILe NPs

3.4 Stability The stability of Amino Acid- Functionalized Gold Nanoparticles

3.4.1 Stability of AA-AuNPs with pH:

The stability of AuNPs under different pH conditions was investigated through experiments conducted at both high and low pH levels. The pH of the AuNPs solution was systematically adjusted using sodium hydroxide for high pH and hydrochloric acid for low pH. AuNPs demonstrate stability at elevated pH levels, whereas they undergo aggregation under low pH conditions. Aggregation of amino acid-functionalized AuNPs as pH varies from high to low is attributed to electrostatic interactions and surface charge changes. It is observed that the pH of the initially synthesized nanoparticle is ~7. The SPR peak of both AuVal and AuIle is at 521 nm, but at low pH, a new peak arises for aggregation along with the SPR peak. At higher pH levels (alkaline conditions), the surface of gold nanoparticles is typically

negatively charged, resulting in repulsion between particles and preventing aggregation. However, as pH decreases (acidic conditions), the surface charge of the gold nanoparticles becomes less harmful or even positive. This reduction in repulsive forces allows attractive van der Waals forces to dominate, leading to particle aggregation. Additionally, variations in pH can influence the solubility of ions in the solution surrounding the nanoparticles, affecting their stability and propensity for aggregation. Therefore, fluctuations in pH from high to low can alter the surface charge and solubility of AA-AuNPs, ultimately driving them to aggregate under conditions where electrostatic repulsion is minimized.

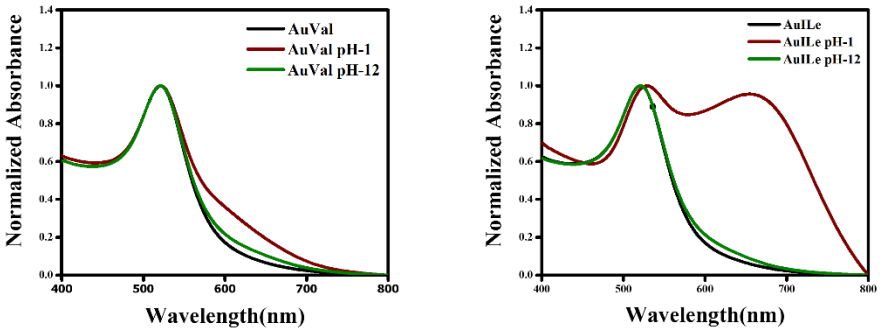

Figure 8: UV-visible spectra of (a) AuVal and (b) AuILe NPs at varying pH.

3.4.2 Stability of AA-AuNPs with Salt:

Upon examining gold nanoparticle stability in the presence of NaCl at a concentration of 0.1 mM, it was revealed that the introduction of NaCl resulted in the aggregation of the nanoparticles. Noticeable aggregation was experienced upon mixing the gold nanoparticle solution with the NaCl solution, indicating a significant impact on the stability of the nanoparticles under the specified NaCl concentration. Aggregation of AA-AuNPs is observed even at 0.1M NaCl concentration due to the screening of repulsive forces and alteration of surface properties induced by the high ionic strength of the salt solution. The SPR peak of both AuVal and AuILe is at 521 nm,

but at low concentrations of NaCl salt, a new peak arises for aggregation along with the SPR peak. Even a low concentration of NaCl ions diminishes the electrostatic repulsion between nanoparticles, allowing attractive van der Waals forces to prevail and leading to particle aggregation. Additionally, the adsorption of Na^+ and Cl^- ions onto the nanoparticle surface can alter the surface chemistry, further promoting aggregation. Consequently, despite the relatively low concentration, 0.1M NaCl still significantly influences the stability of amino acid-functionalized gold nanoparticles, driving them to aggregate.

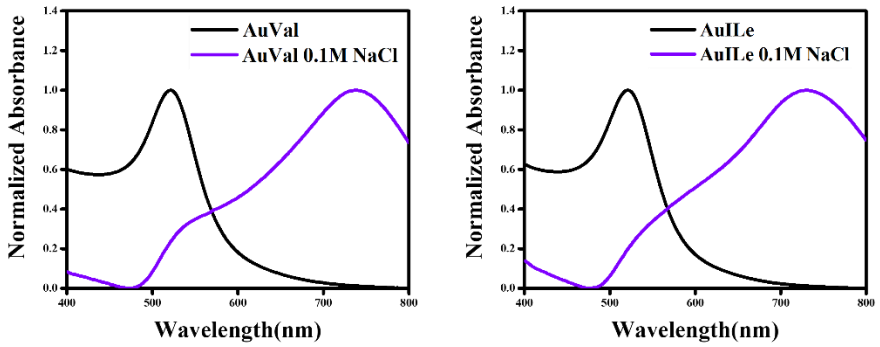

Figure 9: UV-Visible spectra of (a) AuVal and (b) AuILe NPs in the presence of salt.

3.4.3 Stability of AA-AuNPs with Different Metal Ions:

At low concentrations of metal ions, AuNPs remain dispersed and stable, retaining their characteristic SPR peak. With increasing metal ion concentration, a significant shift occurs, resulting in nanoparticle aggregation evidenced by a new broadened peak alongside the SPR peak. This aggregation is likely due to enhanced nanoparticle interactions induced by higher ion concentrations, affecting the electrostatic or steric stabilization forces.

With Ca^{+2} Metal Ion:

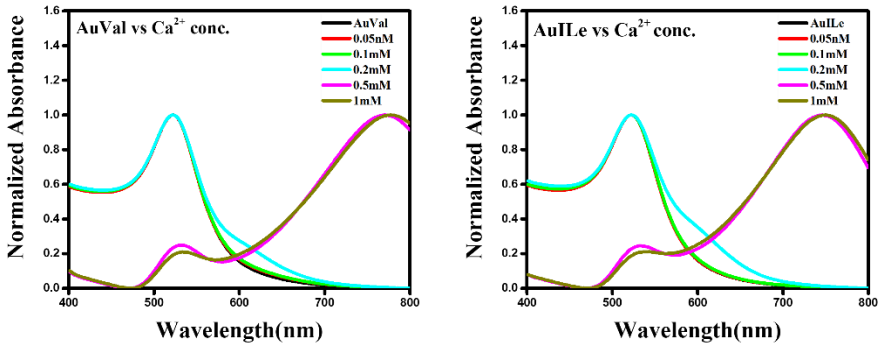

Figure 10: UV-Visible spectra of (a) AuVal and (b) AuILe NPs at varying concentrations of Ca^{+2} Metal Ion.

With Mg^{+2} Metal Ion:

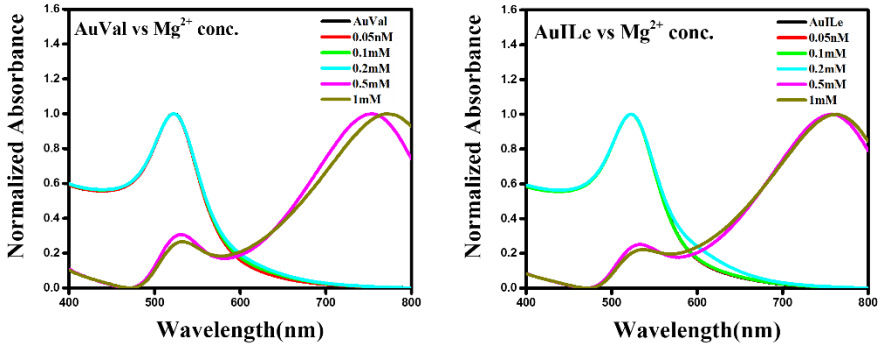

Figure 11: UV-Visible spectra of (a) AuVal and (b) AuILe NPs at varying concentrations of Mg^{+2} Metal Ion.

With Zn^{+2} Metal Ion:

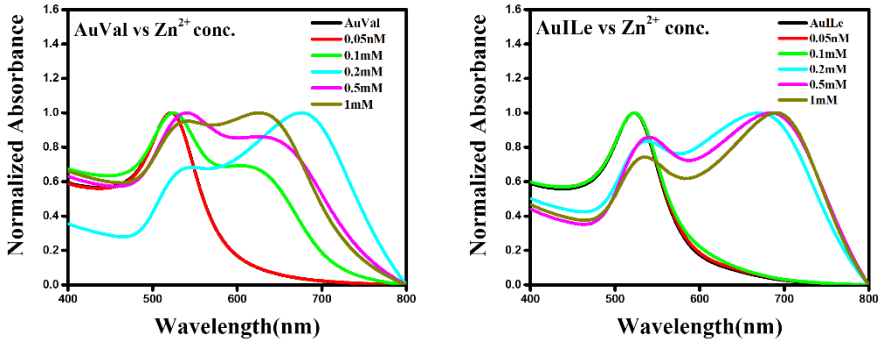

Figure 12: UV-Visible spectra of (a) AuVal and (b) AuILe NPs at varying concentrations of Zn^{+2} Metal Ion.

3.4.4 Stability of AA-AuNPs against freeze-thaw Cycles:

During the freeze-thaw cycle, the nanoparticles with amino acids on their surface start sticking together right from the first cycle. As we repeat the freezing and thawing, they clump together more and more. This shows these nanoparticles do not stay stable when exposed to freeze-thaw conditions. The nanoparticles clump together when frozen and thawed because freezing changes their structure and creates stress from ice formation. Thawing unevenly can also affect how they stick together. The amino acids on the nanoparticle surface may also play a role. Over time, these problems get worse with more freeze-thaw cycles, making the nanoparticles unstable.

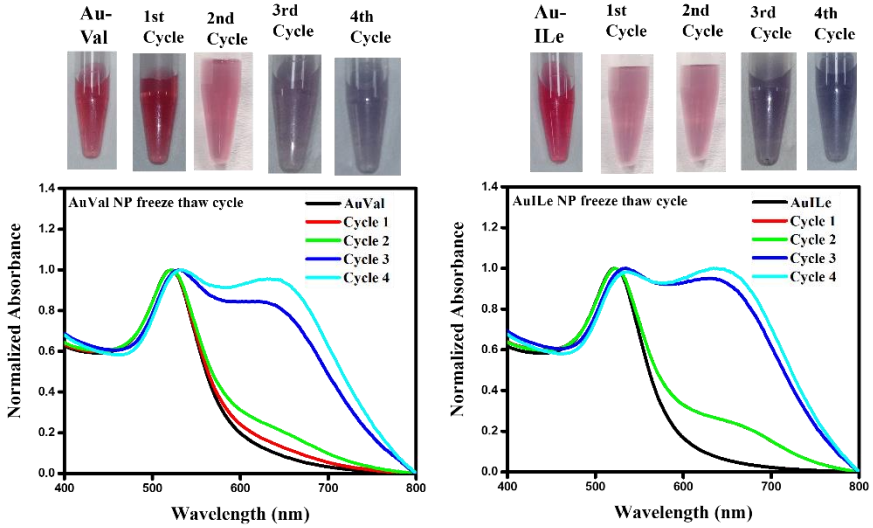

Figure 13: UV-Visible spectra of (a) AuVal and (b) AuILe NPs against freeze-thaw cycles.

3.5 Interaction of Amino Acid-Functionalized AuNPs with HSA Protein

The interaction between amino acid-functionalized gold nanoparticles AuNPs and human serum albumin (HSA) protein is studied to explore how surface functionalization influences protein binding. Amino acid-

functionalized AuNPs strongly interact with HSA protein and form **"Protein Corona."** The SPR peak of AuNPs is at 521 nm, but when interacting with HSA, the spectra shifts by **~6 nm**. Which shows the strong interaction of NP with protein.

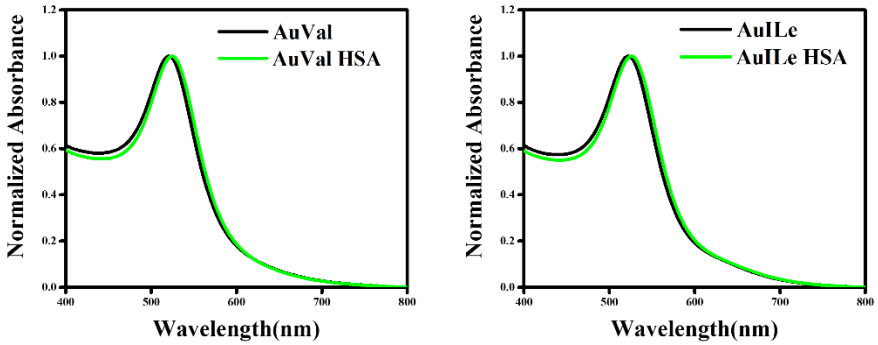

Figure 14: UV-Visible spectra of (a) AuVal and (b) AuILe NPs with HSA.

3.6 Studying the interaction of AuNPs with different Lipid Vesicles

We investigated the interaction of five lipid vesicles having different surface charges, namely DMPC (zwitterionic), DPPC (zwitterionic), DOPC (zwitterionic), DMTAP (positive), and DMPG (negative) With Val and ILe Functionalized AuNPs. We used a 7:3 ratio of DMPC-DMTAP and DMPC/DMPG as the DMTAP and DMPG are charged, whereas the DMPC, DOPC, and DPPC are neutral. We started with 0.8 mM 500 µL of lipid with 500µL 5 nM AuNPs of Val and ILe. We varied the lipid concentration at fixed AuNP concentration to get the desired ratio from 1:1 to 1:160. The lipid-AuNPs mixture was incubated overnight to reach the equilibrium. The UV-Vis absorption spectroscopy was used to establish the interaction.

One key reason is the electrostatic interaction between the charged surface of the NPs and lipid molecule (COO^- group of AuNPs and NR^+_3 group of lipid). At low lipid concentrations, there may not be enough lipid molecules to stabilize the NPs, leading to aggregation. The lipid molecules might also not form a stable lipid bilayer around the NPs, further promoting aggregation. At high concentrations of lipids, more lipid molecules are

available to interact with NPs. Lipid molecules form a stable lipid bilayer around the NPs, creating a **"Lipid Corona."** This corona shields the surface of the NPs and prevents aggregation by providing steric stabilization and reducing the interaction between the NPs themselves. This is the plausible reason for lipid-NP interaction.

3.6.1 AuNPs interaction with zwitterionic lipid vesicles (DMPC):

In the presence of zwitterionic lipid vesicles (DMPC) at high concentrations, both the AuVal and AuILe NPs were stable. However, at low zwitterionic lipid vesicles (DMPC) concentrations, the AuVal and AuILe are a little stable. Still, at medium lipid concentration, both NPs underwent aggregation, and the SPR peak was shifted at a longer wavelength along with a new broadened peak. The UV-Visible spectra showed a spectral shift of SPR peak **~ 9 nm** for AuVal and **~6 nm** for AuILe NPs, whereas the SPR peak was slightly broadened when the lipid concentration was high.

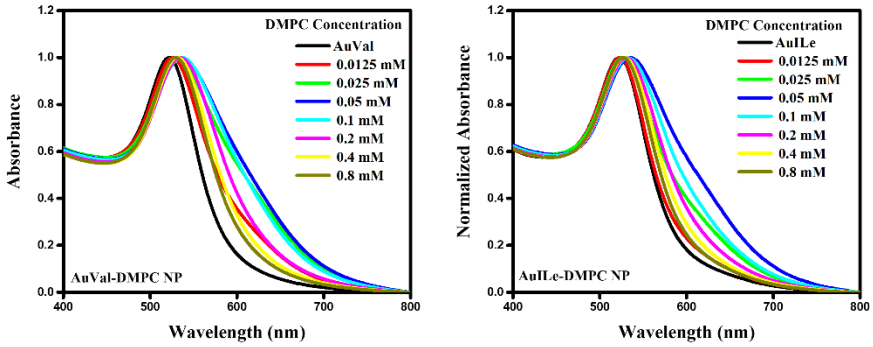

Figure 15: UV-Vis spectra of (a) AuVal and (b) AuILe NPs in the presence of different concentrations of DMPC.

3.6.2 AuNPs interaction with zwitterionic lipid vesicles (DPPC):

In the presence of zwitterionic lipid vesicles (DMPC) at high concentrations, both the AuVal and AuILe NPs were stable. However, at low zwitterionic lipid vesicles (DMPC) concentrations, the AuVal and

AuILe are a little stable. Still, at medium lipid concentration, both NPs underwent aggregation, and the SPR peak was shifted at a longer wavelength along with a new broadened peak. The UV-Visible spectra showed a spectral shift of SPR peak **~7 nm** for AuVal and **~8 nm** for AuILe NPs, whereas the SPR peak was slightly broadened when the lipid concentration was high.

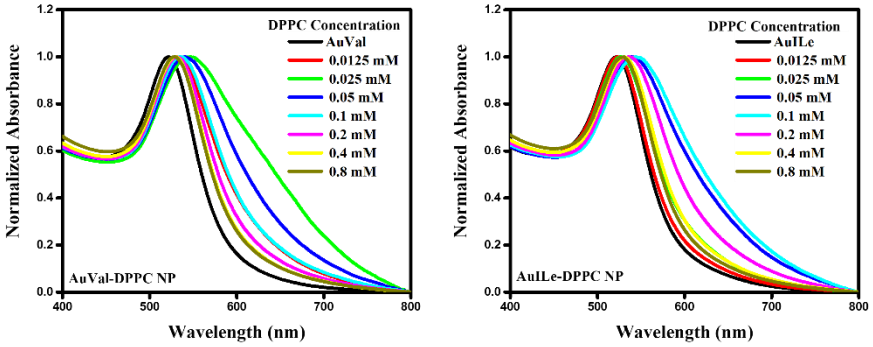

Figure 16: UV-Vis spectra of (a) AuVal and (b) AuILe NPs in the presence of different concentrations of DPPC.

3.6.3 AuNPs interaction with zwitterionic lipid vesicles (DOPC):

In the presence of zwitterionic lipid vesicles (DMPC) at high concentrations, both the AuVal and AuILe NPs were stable. However, at low zwitterionic lipid vesicles (DMPC) concentrations, the AuVal and AuILe are a little stable. Still, at medium lipid concentration, both NPs underwent aggregation, and the SPR peak was shifted at a longer wavelength along with a new broadened peak. The UV-Visible spectra showed a spectral shift of SPR peak **~6 nm** for AuVal and **~6 nm** for AuILe NPs, whereas the SPR peak was slightly broadened when the lipid concentration was high.

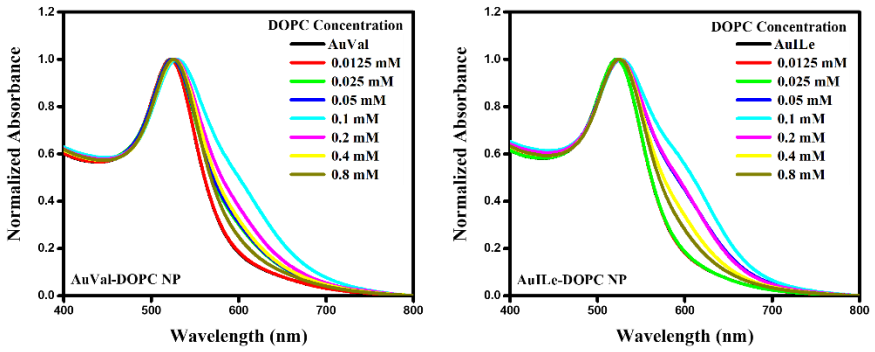

Figure 17: UV-Vis spectra of (a) AuVal and (b) AuILe NPs in the presence of different concentrations of DOPC.

3.6.4 AuNPs interaction with positively charged lipid vesicles (DMPC: DMTAP):

At high concentrations of positively charged lipid vesicles, a significant SPR peak shift was observed in the UV-Visible spectroscopy, approximately **7 nm** for AuVal NP and **8 nm** for AuILe NP from AA-AuNPs, with an SPR peak of 521 nm. As the lipid concentration decreased, AuVal and AuILe NPs underwent aggregation, suggesting lipid-induced aggregation. This implies aggregates are formed when NP numbers exceed positive-charged lipid molecules, which are not sufficient, indicating their sensitivity to lipid concentration.

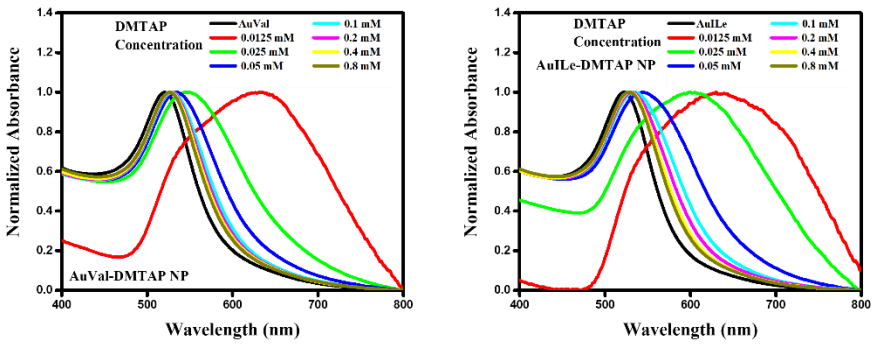

Figure 18: UV-Vis spectra of (a) AuVal and (b) AuILe NPs in the presence of different concentrations of DMTAP.

3.6.5 AuNPs interaction with negatively charged lipid vesicles (DMPC: DMPG):

The UV-Visible spectra showed that the AuVal and AuILe NPs did not interact with negatively charged lipid vesicles at any concentration, as the SPR peak was not shifted. The results suggested that the AuNPs are negatively charged.

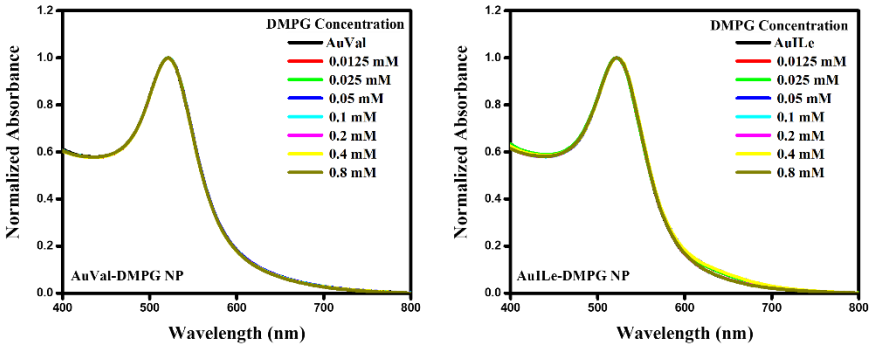

Figure 19: UV-Vis spectra of (a) AuVal and (b) AuILe NPs in the presence of different concentrations of DMPG.

3.7 Studying the Effect of Lipid Coating on the Stability of AuNPs

The impact of lipid coating on the stability of NPs was examined by combining 500 µL of 5 nM NPs with 500 µL of liposomes containing various lipids at a concentration of 0.8 mM. At specific pH levels and in the presence of varied ion concentrations and the addition of various quantities of NaCl, the stability of NPs decreases; however, compared to naked NPs, lipid-coated NPs are far more stable because the lipid coating increases biocompatibility and protects them from the hostile environment of biological fluid. Finally, a freeze-thaw cycle was performed, maintaining the solution at -20°C during freezing and allowing it to thaw at room temperature. It was observed that the lipid coating offered an exceptional degree of durability to the NPs. The interaction was analyzed using UV-Vis absorption spectroscopy.

3.7.1 Stability of lipid-coated AuNPs against pH:

Lipid-coated AuNPs are stable against pH changes primarily because the lipid layer surrounding them acts as a protective barrier. This lipid shield prevents the AuNPs from aggregating or clumping together when the pH of the surrounding environment shifts. In contrast, amino acid-functionalized AuNPs lack this protective layer and are more susceptible to aggregation under acidic or basic conditions. Additionally, the lipids can help stabilize the pH around the nanoparticles, maintaining a more consistent environment that further supports nanoparticle stability.

DMPC Coated AuNPs:

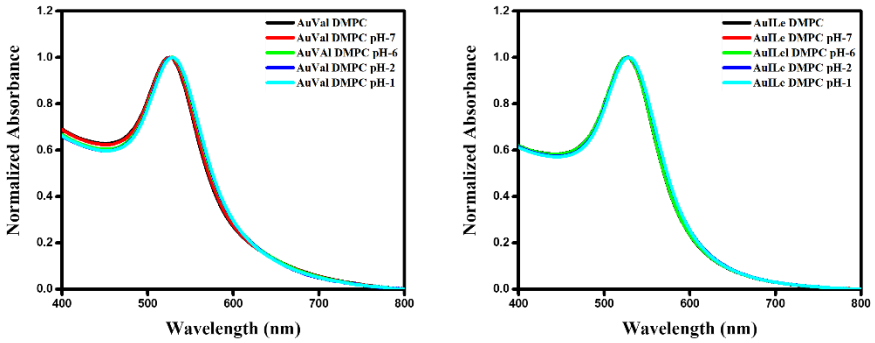

Figure 20: UV-Vis spectra of DMPC coated (a) AuVal and (b) AuILe NPs at different pH.

DPPC Coated AuNPs:

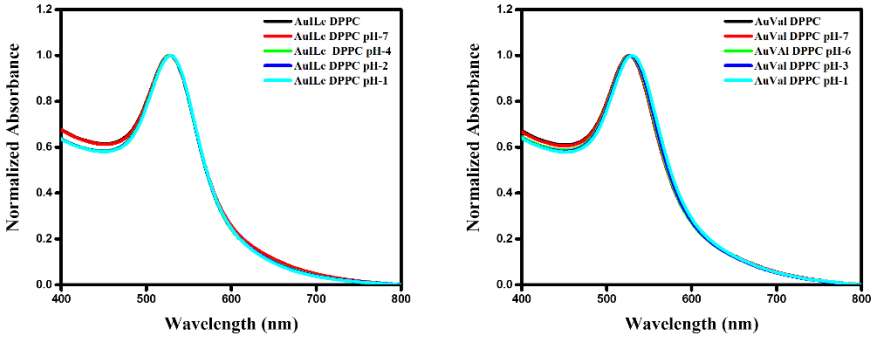

Figure 21: UV-Vis spectra of DPPC coated (a) AuVal and (b) AuILe NPs at different pH.

DOPC Coated AuNPs:

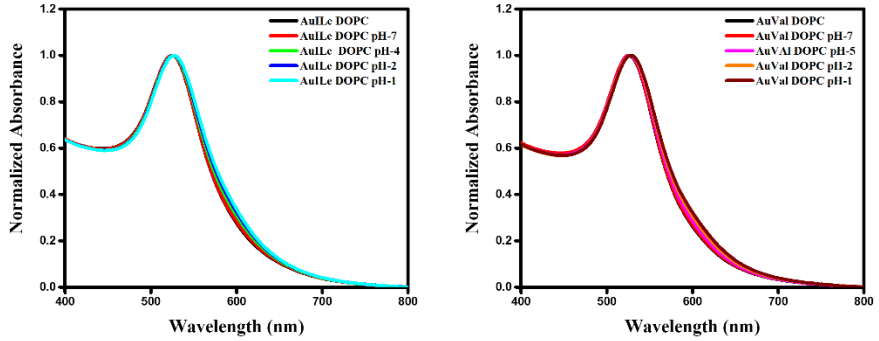

Figure 22: UV-Vis spectra of DOPC coated (a) AuVal and (b) AuILe NPs at varying pH.

DMTAP Coated AuNPs:

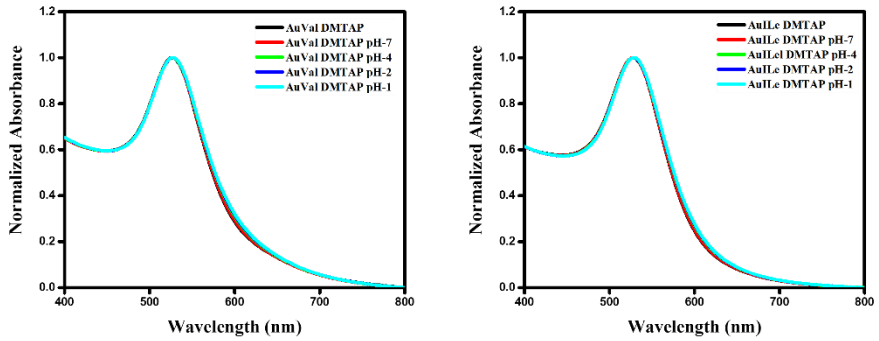

Figure 23: UV-Vis spectra of DMTAP coated (a) AuVal and (b) AuILe NPs at varying pH.

3.7.2 Stability of lipid-coated AuNPs against NaCl Salt:

Lipid-coated AuNPs maintain stability against NaCl salt due to the protective lipid layer surrounding them. This lipid coating acts as a shield, preventing the AuNPs from clumping together (aggregating) in the presence of salt. The lipids create a barrier that reduces the impact of salt ions on the AuNP surface, preserving their dispersed state. In contrast, amino acid-functionalized AuNPs are more prone to aggregation at low concentrations of salt conditions because they lack this protective coating.

DMPC Coated AuNPs:

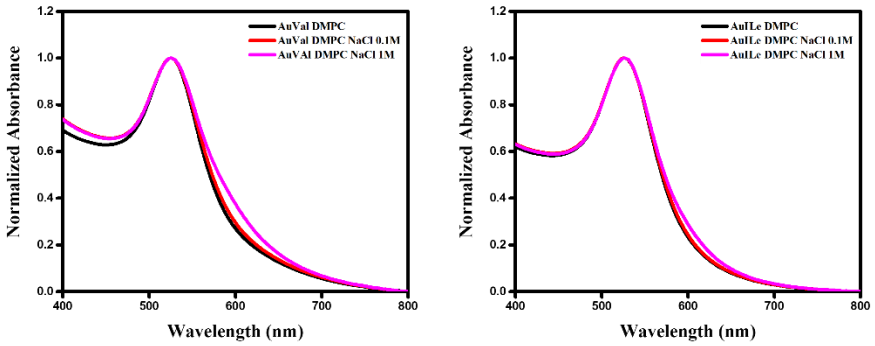

Figure 24: UV-Vis spectra of DMPC coated (a) AuVal and (b) AuILe NPs at varying salt concentrations.

DPPC Coated AuNPs:

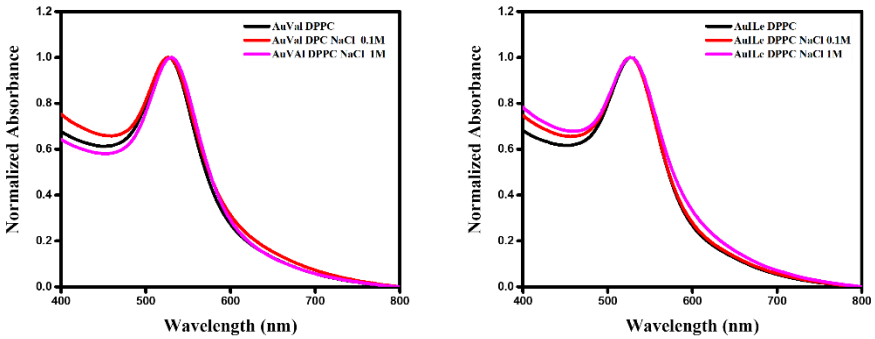

Figure 25: UV-Vis spectra of DPPC coated (a) AuVal and (b) AuILe NPs at varying salt concentrations.

DOPC Coated AuNPs:

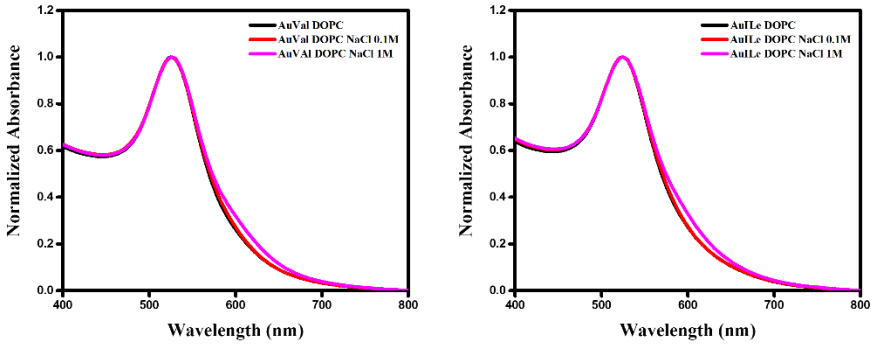

Figure 26: UV-Vis spectra of DOPC coated (a) AuVal and (b) AuILe NPs at varying salt concentrations.

DMTAP Coated AuNPs:

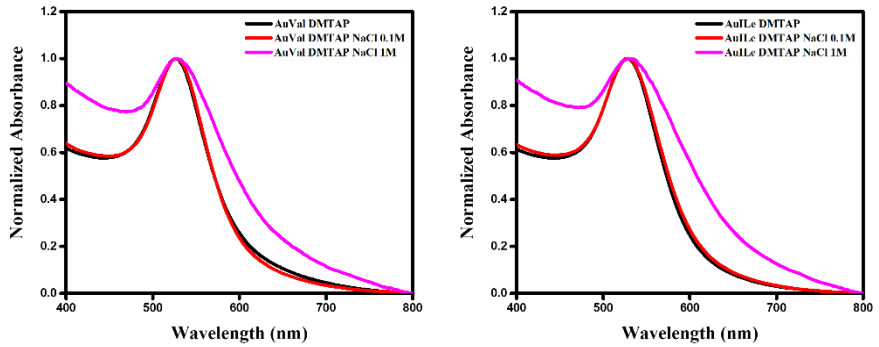

Figure 27: UV-Vis spectra of DMTAP coated (a) AuVal and (b) AuILe NPs at varying salt concentrations.

3.7.3 Stability of lipid-coated AuNPs against Freeze-thaw cycles:

In the freeze-thaw cycle, the amino acid functionalized NP seems to be involved in aggregation from the first cycle. Meanwhile, the lipid-coated NP does not undergo aggregation. We did four freeze-thaw cycles, out of which there was no lipid-coated NP aggregation in any of the freeze-thaw cycles. This shows that our Lipid-coated NP is stable against freeze-thaw throughout multiple cycles.

DMPC Coated AuNPs against freeze-thaw cycle:

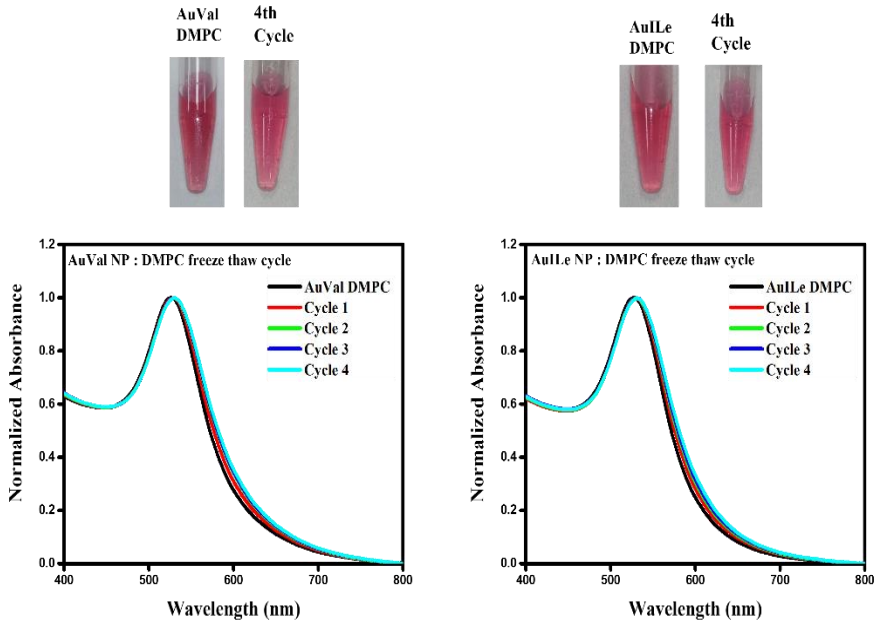

Figure 28: UV-Vis spectra of DMPC coated (a) AuVal and (b) AuILe NPs against freeze-thaw cycles.

DPPC Coated AuNPs against freeze-thaw cycle:

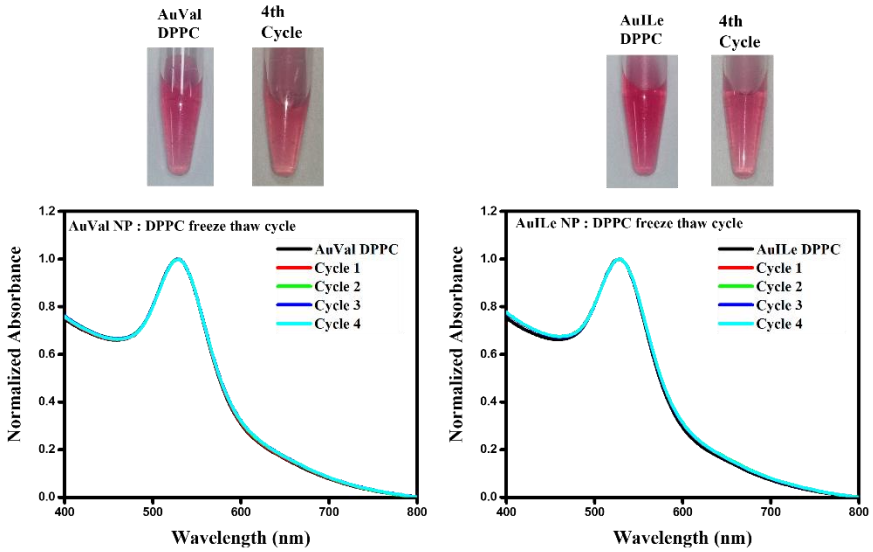

Figure 29: UV-Vis spectra of DPPC coated (a) AuVal and (b) AuILe NPs against freeze-thaw cycles.

DOPC Coated AuNPs against freeze-thaw cycle:

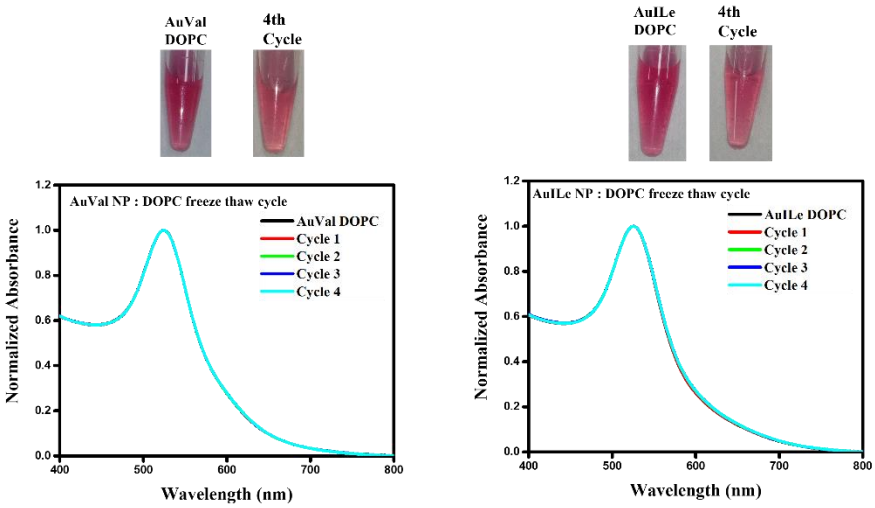

Figure 30: UV-Vis spectra of DOPC coated (a) AuVal and (b) AuILe NPs against freeze-thaw cycles.

DMTAP Coated AuNPs against freeze-thaw cycle:

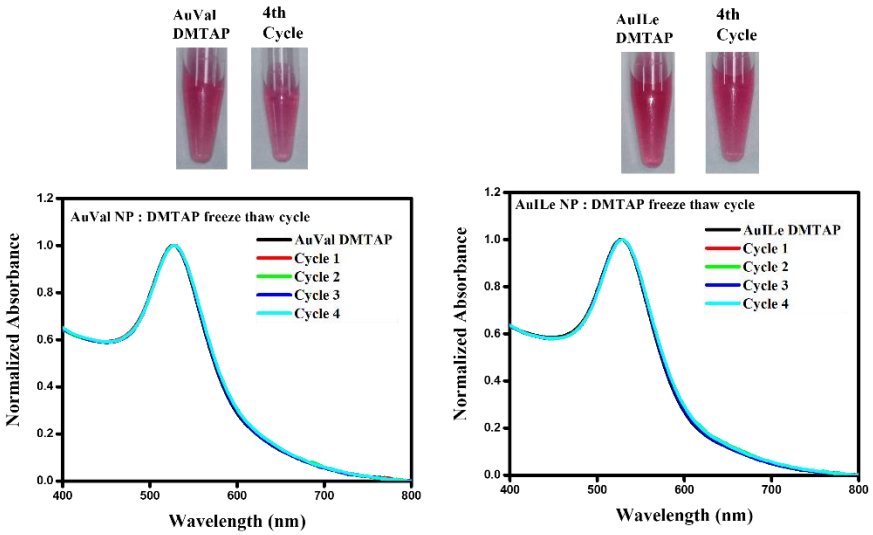

Figure 31: UV-Vis spectra of DMTAP coated (a) AuVal and (b) AuILe NPs against freeze-thaw cycles.

3.8 Interaction of Lipid-Coated AuNPs with Protein

The absence of a biological corona on lipid-coated gold nanoparticles can be attributed to the protective barrier formed by the lipid layer. This layer shields the gold surface, hindering direct protein interactions. Lipid composition, surface charge, and nanoparticle stability influence this behavior. The stable lipid coating prevents exposure of the gold surface, reducing protein adsorption.

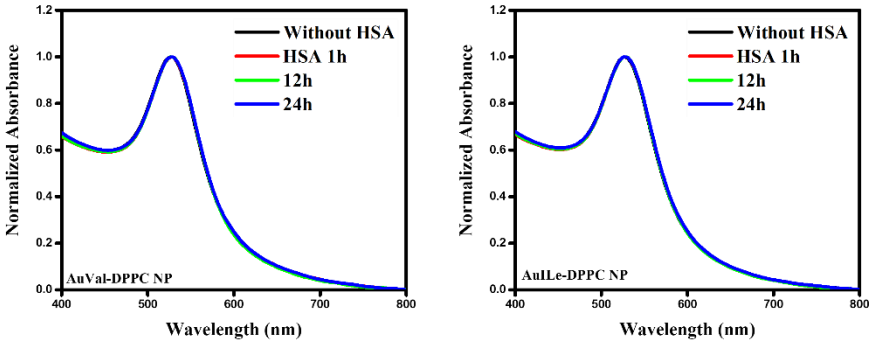

Figure 32: UV-Vis spectra of DOPC coated (a) AuVal and (b) AuILe NPs with HSA.

Supporting Information

The lipid-nanoparticle mixture was centrifuged to remove excess lipids that might affect the stability of lipid-coated AuVal and AuILe NPs. After centrifugation, the supernatant containing unbound lipids was discarded, and the pellet was then resuspended in a HEPES buffer (the centrifuge process was discussed earlier). This process improves NP stability by removing excess lipids and ensures the reliability of future experiments or applications involving these lipid-coated nanoparticles. Again, we performed the pH, salt, and freeze-thaw experiments on the after-centrifuged lipid-coated NPs to check whether they were stable like before or if something happened after the centrifugation of lipid-coated NPs.

Stability of Lipid-coated AuNPs against pH (After Centrifuge):

Both AuNPs are stable after centrifugation against pH. No broadening in the SPR peak was noted after centrifugation of the lipid-coated AuVal and AuILe NPs. This suggests that excess lipids were effectively removed through the purification process, with minimal impact on the optical properties or stability of the nanoparticles.

DMPC Coated AuNPs against pH (After Centrifuge):

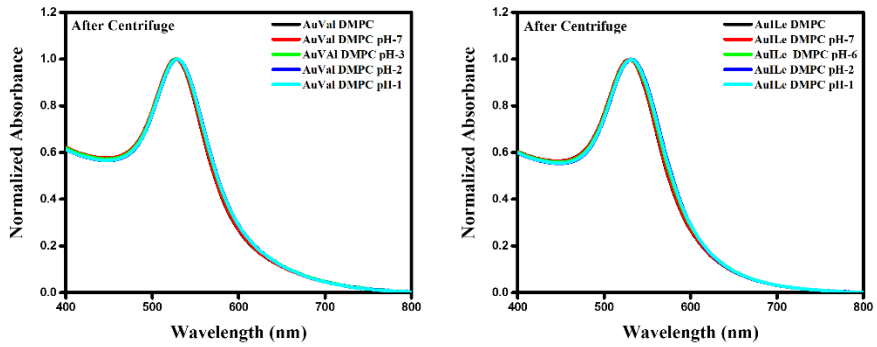

Figure 33: UV-Vis spectra of DMPC coated (a) AuVal and (b) AuILe NPs at different pH (After Centrifuge).

DPPC Coated AuNPs against pH (After Centrifuge):

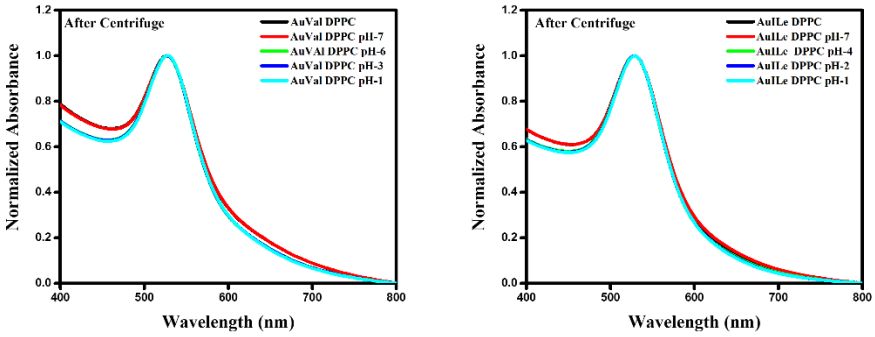

Figure 34: UV-Vis spectra of DPPC coated (a) AuVal and (b) AuILe NPs at different pH (After Centrifuge).

DOPC Coated AuNPs against pH (After Centrifuge):

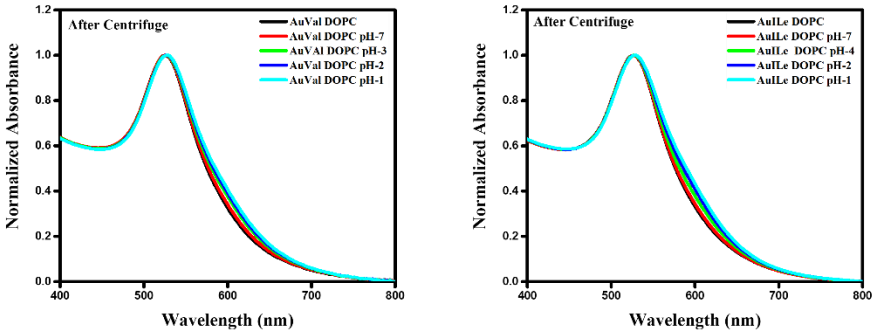

Figure 35: UV-Vis spectra of DOPC coated (a) AuVal and (b) AuILe NPs at different pH (After Centrifuge).

DMTAP Coated AuNPs against pH (After Centrifuge):

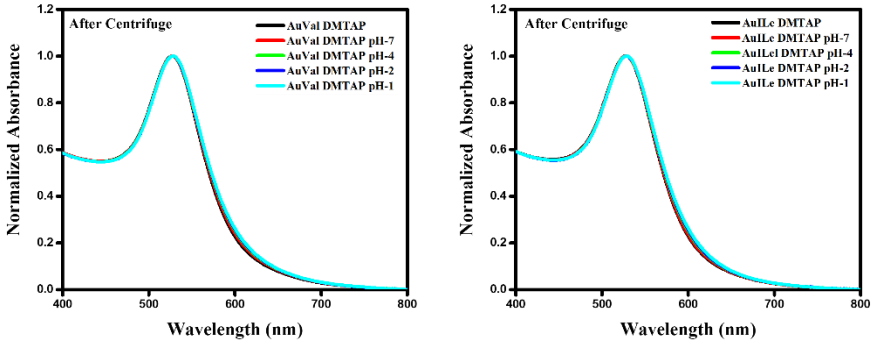

Figure 36: UV-Vis spectra of DMTAP coated (a) AuVal and (b) AuILe NPs at different pH (After Centrifuge).

Stability of Lipid-coated AuNPs against Salt (After Centrifuge):

Both AuNPs are stable after centrifugation against Salt. No broadening in the SPR peak was noted after centrifugation of the lipid-coated AuVal and AuILe NPs for DPPC and DOPC. Still, there is a little bit less stability at high concentrations of NaCl salt in the case of DMTAP lipid for both AuNPs and DMPC lipid for AuILe NP. This suggests that excess lipids were effectively removed through the purification process, with minimal impact on the optical properties or stability of the nanoparticles.

DMPC Coated AuNPs against salt (After Centrifuge):

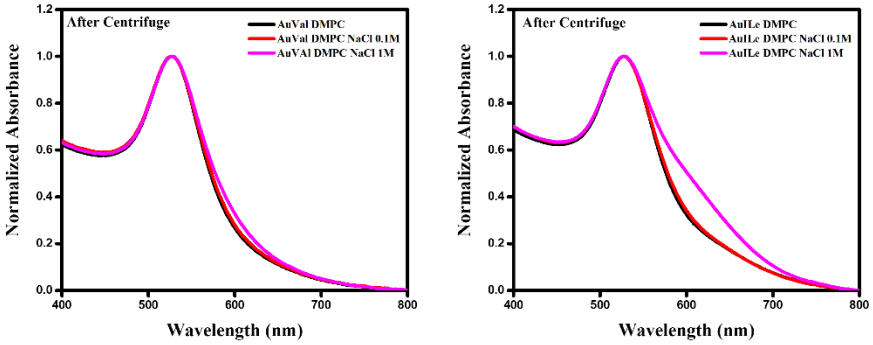

Figure 37: UV-Vis spectra of DMPC coated (a) AuVal and (b) AuILe NPs at different salt concentrations (After Centrifuge).

DPPC Coated AuNPs against salt (After Centrifuge):

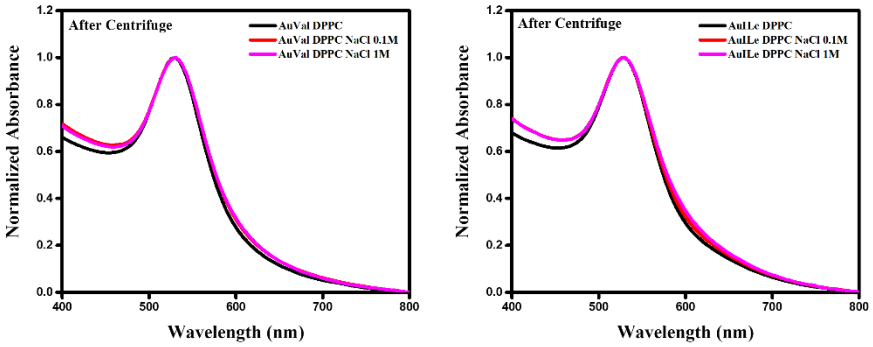

Figure 38: UV-Vis spectra of DPPC coated (a) AuVal and (b) AuILe NPs at different salt concentrations (After Centrifuge).

DOPC Coated AuNPs against salt (After Centrifuge):

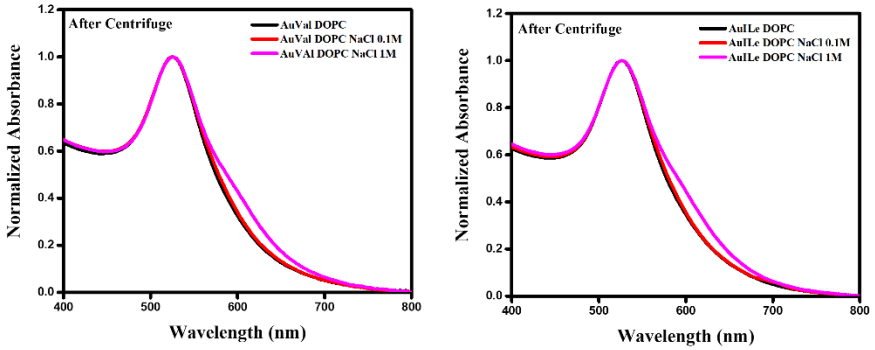

Figure 39: UV-Vis spectra of DOPC coated (a) AuVal and (b) AuILe NPs at different salt concentrations (After Centrifuge).

DMTAP Coated AuNPs against salt (After Centrifuge):

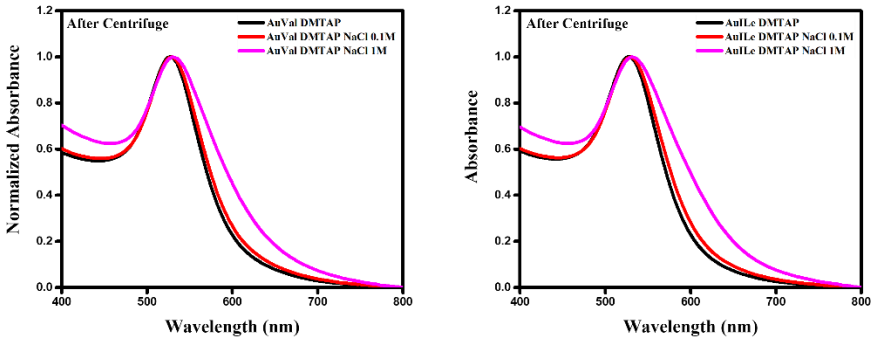

Figure 40: UV-Vis spectra of DMTAP coated (a) AuVal and (b) AuILe NPs at different salt concentrations (After Centrifuge).

Stability of lipid-coated AuNPs against Freeze-thaw cycle (After Centrifuge):

Even after centrifugation, all the nanoparticles remained stable against freeze-thaw. This suggests that excess lipids were effectively removed through the purification process, with minimal impact on the optical properties or stability of the nanoparticles.

DMPC Coated AuNPs against freeze-thaw cycle (After Centrifuge):

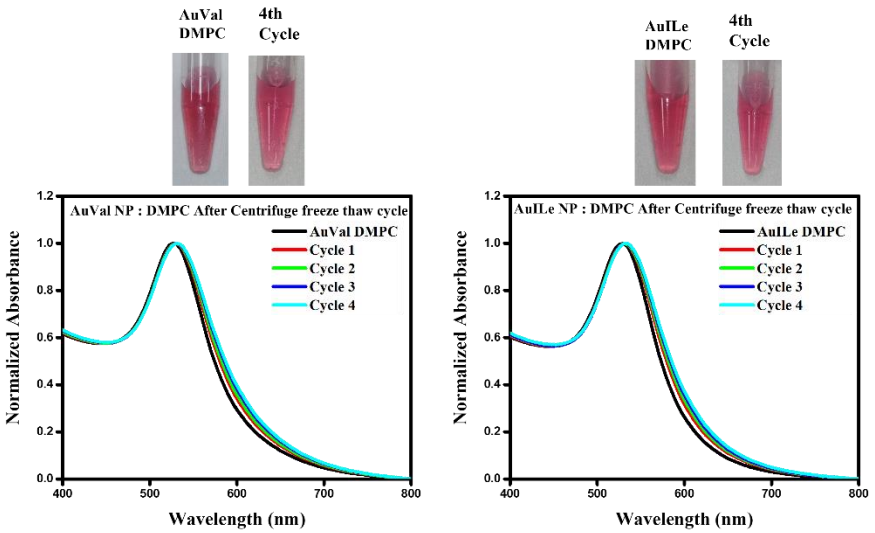

Figure 41: UV-Vis spectra of DMPC coated (a) AuVal and (b) AuILe NPs against freeze-thaw cycles (After Centrifuge).

DPPC Coated AuNPs against freeze-thaw cycle (After Centrifuge):

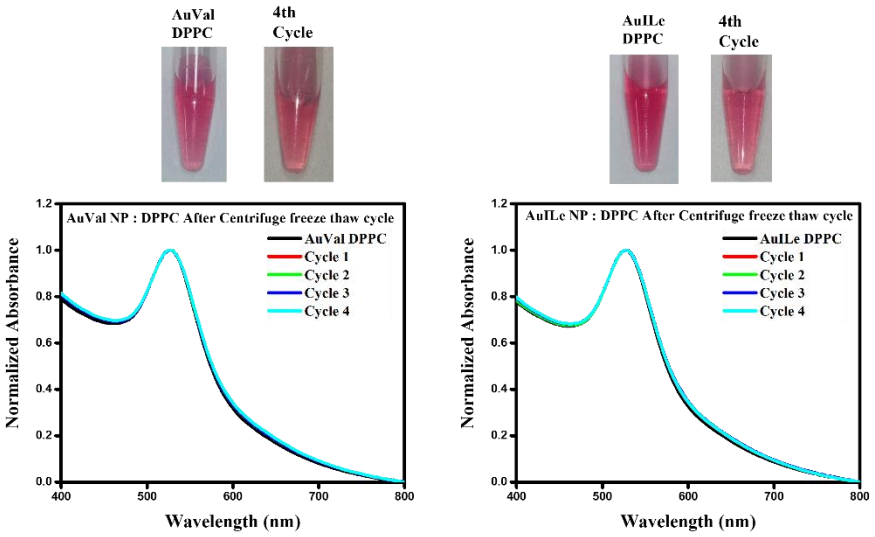

Figure 42: UV-Vis spectra of DPPC coated (a) AuVal and (b) AuILe NPs against freeze-thaw cycles (After Centrifuge).

DOPC Coated AuNPs against freeze-thaw cycle (After Centrifuge):

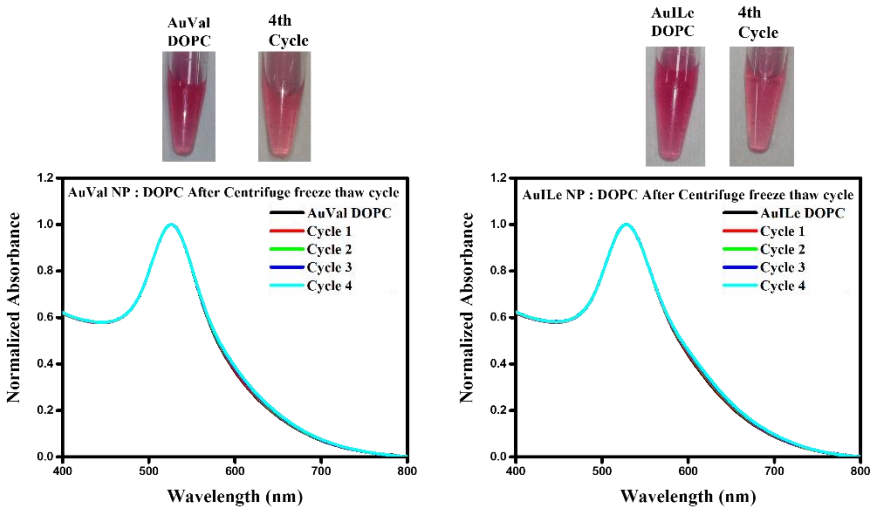

Figure 43: UV-Vis spectra of DOPC coated (a) AuVal and (b) AuILe NPs against freeze-thaw cycles (After Centrifuge).

DMTAP Coated AuNPs against freeze-thaw cycle (After Centrifuge):

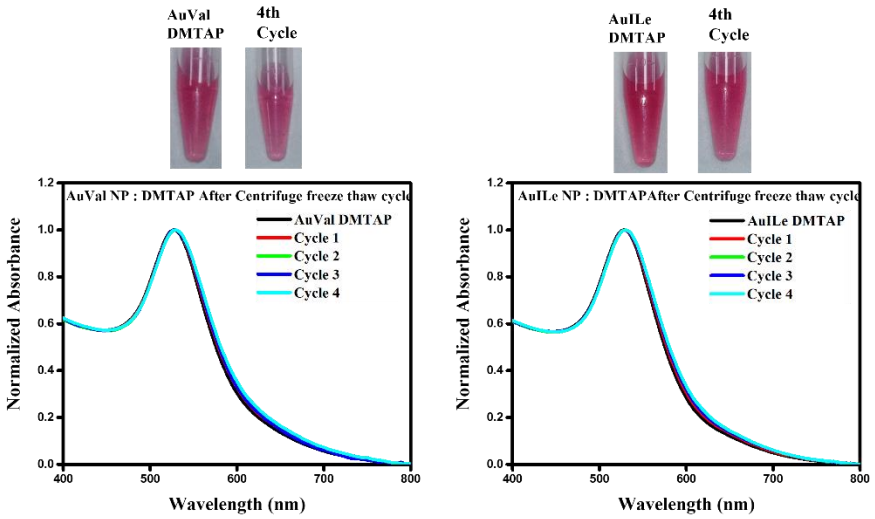

Figure 44: UV-Vis spectra of DMTAP coated (a) AuVal and (b) AuILe NPs against freeze-thaw cycles (After Centrifuge).

Structure of Lipids

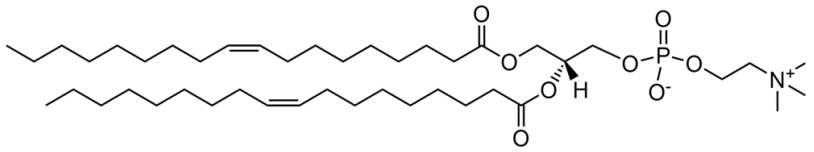

DOPC

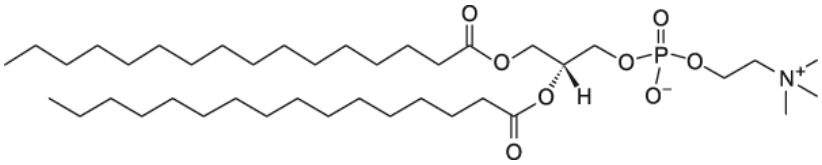

DPPC

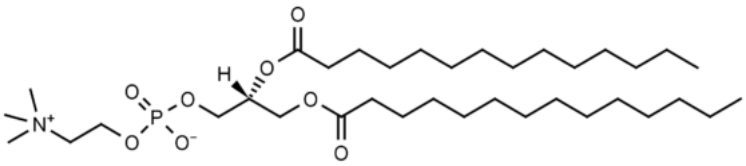

DMPC

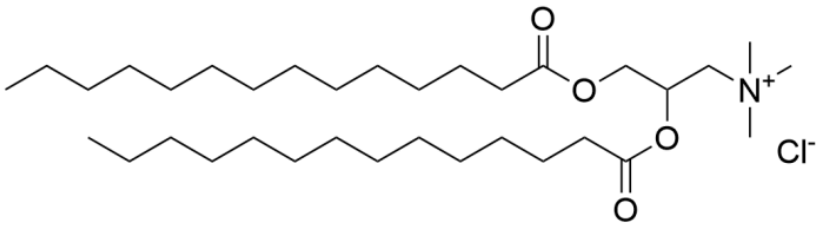

DMTAP

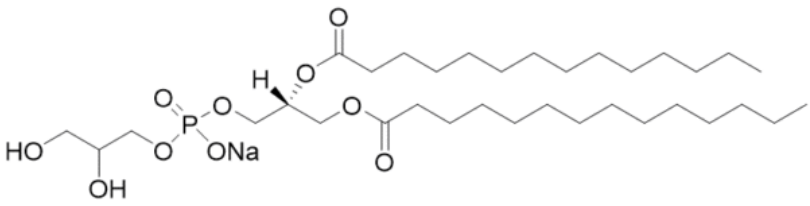

DMPG

Conclusions

Herein, we have synthesized valine and isoleucine functionalized gold nanoparticles and then investigated the stability of nanoparticles in different mediums. We also studied the interaction of synthesized gold nanoparticles with different surface-charged lipid vesicles. We analyzed how the Lipid coating around the AA-AuNPs can affect its stability. We draw the following conclusions from our observations.

a) We have successfully optimized the reaction condition to synthesize valine and isoleucine functionalized gold nanoparticles.
b) We checked the stability of the nanoparticles after synthesis in different conditions.
c) We have investigated the interaction of valine and isoleucine functionalized gold nanoparticles with differently surface-charged lipid vesicles.
d) Initially, valine and isoleucine functionalized AuNPs unstable against external stimuli like pH and salt. These NPs aggregated in low pH conditions and low salt concentrations when we performed a stability study with these experiments.
e) Valine and Isoleucine are functionalized, interacting with the protein and forming a Protein Corona.
f) Valine and Isoleucine functionalized gold nanoparticles are stable with zwitterionic lipids at high concentrations and lipid vesicles with positive charges. It undergoes aggregation with lipids having positive and zwitterionic charges at low concentrations.
g) Valine and Isoleucine functionalized silver nanoparticles do not interact with negatively charged lipid vesicles, suggesting that the nanoparticles are negatively charged.
h) Lipid-coated AuNPs do not interact with proteins, indicating that the surface modification on the molecules is stable even under biological conditions.

i) The nanoparticles that exhibit significant interactions with various lipids have lipid molecules coating their surfaces, which boosts their durability to a greater extent by protecting them from the severe conditions found in biological fluids.

References

1) Pearson, R.M., Juettner, V.V. and Hong, S., 2014. Biomolecular corona on nanoparticles: a survey of recent literature and its implications in targeted drug delivery. Frontiers in chemistry, 2, 108.
2) Pozzi, D., Colapicchioni, V., Caracciolo, G., Piovesana, S., Capriotti, A.L., Palchetti, S., De Grossi, S., Riccioli, A., Amenitsch, H. and Laganà, A., 2014. Effect of polyethyleneglycol chain length on the bio–nano-interactions between PEGylated lipid nanoparticles and biological fluids: from nanostructure to uptake in cancer cells. Nanoscale, 6, 2782-2792.
3) Moyano, D.F., Saha, K., Prakash, G., Yan, B., Kong, H., Yazdani, M. and Rotello, V.M., 2014. Fabrication of corona-free nanoparticles with tunable hydrophobicity. ACS nano, 8, 6748-6755.
4) Zhang, X., Pandiakumar, A.K., Hamers, R.J. and Murphy, C.J., 2018. Quantification of lipid corona formation on colloidal nanoparticles from lipid vesicles. Analytical chemistry, 90, 14387-14394.
5) Magar, K.T., Boafo, G.F., Li, X., Chen, Z. and He, W., 2022. Liposome-based delivery of biological drugs. Chinese Chemical Letters, 33, 587-596.
6) Maity, A., De, S.K. and Chakraborty, A., 2021. Interaction of Aromatic Amino Acid-Functionalized Gold Nanoparticles with Lipid Bilayers: Insight into the Emergence of Novel Lipid Corona Formation. The Journal of Physical Chemistry B, 125, 2113-2123.
7) Tabassum, H., Maity, A., Singh, K., Bagchi, D., Prasad, A. and Chakraborty, A., 2024. Effect of Lipid Corona on Phenylalanine-Functionalized Gold Nanoparticles to Develop Stable and Corona-Free Systems. Langmuir, 40, 4531-4543

8) Maity, A., Nath, P., Bagchi, D., Debnath, S., Tabassum, H., Sinha, S. and Chakraborty, A., 2024. Formation of lipid corona on Ag nanoparticles and its impact on Ag+ ion dissolution and aggregation of Ag nanoparticles against external stimuli. Chemical Physics Impact, 8, 100445.
9) Hough, R.M., Noble, R.R.P. and Reich, M., 2011. Natural gold nanoparticles. Ore Geology Reviews, 42, 55-61.
10) Arvizo, R., Bhattacharya, R. and Mukherjee, P., 2010. Gold nanoparticles: opportunities and challenges in nanomedicine. Expert opinion on drug delivery, 7, 753-763.
11) Amendola, V. and Meneghetti, M., 2009. Size evaluation of gold nanoparticles by UV− vis spectroscopy. The Journal of Physical Chemistry C, 113, 4277-4285.
12) Jennings, T. and Strouse, G., 2007. Past, present, and future of gold nanoparticles. Bio-Applications of Nanoparticles, 2, 34-47.
13) Zhang, G., 2013. Functional gold nanoparticles for sensing applications. Nanotechnology Reviews, 2, 269-288.
14) Giljohann, D.A., Seferos, D.S., Daniel, W.L., Massich, M.D., Patel, P.C. and Mirkin, C.A., 2020. Gold nanoparticles for biology and medicine. Spherical Nucleic Acids, 4, 55-90.
15) Madkour, L.H., 2018. Applications of gold nanoparticles in medicine and therapy. Pharm. Pharmacol. Int. J, 6, 157-174.
16) Daraee, H., Eatemadi, A., Abbasi, E., Fekri Aval, S., Kouhi, M. and Akbarzadeh, A., 2016. Application of gold nanoparticles in biomedical and drug delivery. Artificial cells, nanomedicine, and biotechnology, 44, 410-422.
17) Schmid, G. and Corain, B., 2003. Nanoparticulated gold: syntheses, structures, electronics, and reactivities. European Journal of Inorganic Chemistry, 37, 3081-3098.

18) Liu, G., Lin, Y., Ostatná, V. and Wang, J., 2005. Enzyme nanoparticles-based electronic biosensor. Chemical communications, 27, 3481-3483.
19) Qian, H., Pretzer, L.A., Velazquez, J.C., Zhao, Z. and Wong, M.S., 2013. Gold nanoparticles for cleaning contaminated water. Journal of Chemical Technology & Biotechnology, 88, 735-741.
20) Hitchman, A., Smith, G.H.S., Ju-Nam, Y., Sterling, M. and Lead, J.R., 2013. The effect of environmentally relevant conditions on PVP stabilised gold nanoparticles. Chemosphere, 90, 410-416.
21) Fuller, M.A. and Köper, I., 2019. Biomedical applications of polyelectrolyte coated spherical gold nanoparticles. Nano convergence, 6, 11.
22) Datta, D., Deepak, K.S. and Das, B., 2022. Progress in the synthesis, characterisation, property enhancement techniques and application of gold nanoparticles: A review. MRS Communications, 12, 700-715.
23) Tomar, A. and Garg, G., 2013. Short review on application of gold nanoparticles. Global Journal of Pharmacology, 7, 34-38.
24) De Souza, C.D., Nogueira, B.R. and Rostelato, M.E.C., 2019. Review of the methodologies used in the synthesis gold nanoparticles by chemical reduction. Journal of Alloys and Compounds, 798, 714-740.
25) Nikoobakht, B. and El-Sayed, M.A., 2003. Preparation and growth mechanism of gold nanorods using seed-mediated growth method. Chemistry of materials, 15, 1957-1962.
26) Santhosh, P.B., Genova, J. and Chamati, H., 2022. Green synthesis of gold nanoparticles: An eco-friendly approach. Chemistry, 4, 345-369.
27) Hasan, S., 2015. A review on nanoparticles: their synthesis and types. Res. J. Recent Science, 2277, 2502.

28) Stetefeld, J., McKenna, S.A. and Patel, T.R., 2016. Dynamic light scattering: a practical guide and applications in biomedical sciences. Biophysical reviews, 8, 409-427.
29) Bhattacharjee, S., 2016. DLS and zeta potential–what they are and what they are not?. Journal of controlled release, 235, 337-351.
30) Nagle, J.F. and Tristram-Nagle, S., 2000. Lipid bilayer structure. Current opinion in structural biology, 10, 474-480.
31) Magar, K.T., Boafo, G.F., Li, X., Chen, Z. and He, W., 2022. Liposome-based delivery of biological drugs. Chinese Chemical Letters, 33, 587-596.
32) Jackman, J.A., Knoll, W. and Cho, N.J., 2012. Biotechnology applications of tethered lipid bilayer membranes. Materials, 5, 2637-2657.
33) Xu, F., Reiser, M., Yu, X., Gummuluru, S., Wetzler, L. and Reinhard, B.M., 2016. Lipid-mediated targeting with membrane-wrapped nanoparticles in the presence of corona formation. ACS nano, 10, 1189-1200.
34) Jang, G.J., Jeong, J.Y., Kang, J., Cho, W. and Han, S.Y., 2021. Size dependence unveiling the adsorption interaction of high-density lipoprotein particles with PEGylated gold nanoparticles in biomolecular corona formation. Langmuir, 37, 9755-9763.
35) Olenick, L.L., Troiano, J.M., Vartanian, A., Melby, E.S., Mensch, A.C., Zhang, L., Hong, J., Mesele, O., Qiu, T., Bozich, J. and Lohse, S., 2018. Lipid corona formation from nanoparticle interactions with bilayers. Chem, 4, 2709-2723.
36) Zhang, L., Li, P., Li, D., Guo, S. and Wang, E., 2008. Effect of freeze-thawing on lipid bilayer-protected gold nanoparticles. Langmuir, 24, 3407-3411.